ISSN 2706-7726

# AZERBAIJAN UNIVERSITY OF ARCHITECTURE ANDCONSTRUCTION

# ENGINEERING MECHANICS

№ 2

September 2023

Azerbaijan University of Architecture and Construction
ISSN 2706-7726

Engineering Mechanics
Scientific and Technical Journal

E-mail: engineeringmechanics@azmiu.edu.az

September 2023 Issue 14 Volume 6 Number 2

## CONTENTS

Azerbaijan University of Architecture and Construction
ISSN 2706-7726
Engineering Mechanics
Scientific and Technical Journal
E-mail: engineeringmechanics@azmiu.edu.az

| September 2023 | Issue 14 | Volume 6 | Number 2 | Pages 3-5 |
|---|---|---|---|---|

# SPHERICAL INSERT WITH ELASTICALLY FIXED MASS STUDY OF MOTION IN A SOLID ELASTIC MEDIUM

**F.A.SEYFULLAEV, N.I.HASANOV**
*Institute of Mathematics and Mechanics of the Ministry of Science and Education of the Republic of Azerbaijan*
kur_araz@rambler.ru

**Abstract:** *Issues devoted to the non-stationary interaction of deformable and solid bodies with the environment are of great theoretical and practical importance. The study of movements and dances of structures interacting with the environment is one of the most pressing problems of our time. The experience of modern fields of mechanical engineering and construction requires studying the impact of shock waves propagating in the environment surrounding the body on elements of structures and buildings.This applies, first of all, to the design of aircraft, underwater and surface structures, ships, public and industrial structures with large floors. At this time, the construction and reporting of these objects is carried out, on the one hand, from the point of view of assessing their strength, and on the other hand, in order to determine the speed and acceleration created in them due to the impact of impact loads, therefore, in addition to the strength of the object, the designer uses the available he has the equipment for the necessary work.*

In this regard, a classification of classical problems of this type has developed in mechanics.

Various issues related to bodies and structures that interact unsteadily with the entire environment are covered in monographs [1,2,3] and other literature. In most studies of the interaction of waves with obstacles, the main interest is in the kinematic parameters characterizing the displacement of the center of mass of the body. In this case, the elasticity of the body is usually not taken into account and it is considered as an absolutely rigid body. Determining the load when a rigid body moves according to a given law is the initial stage of solving the problem of interaction of a moving obstacle with the environment. Based on the Laplace transform in time, this issue was considered in monographs.

The paper examines the influence of a system of loads located inside and in mutual contact with spherical waves on the state of a cylindrical shell. The load system (grouped masses) is attached to the inner surface of the cover by means of elastic springs. The masses are also connected to each other through elastic springs with linear characteristics. The crowd can only move forward and backward. The solution to the problem is constructed using Fourier series (in terms of angular coordinates) and integral transformations (in Laplacian time in terms of Fourier axis coordinates). Copy integrals were calculated using the Gauss-Laguerre quadratic formula (for Fourier transform transforms) and using ultraspherical polynomials without serialization (for Laplace transform transforms). Numerical calculations were carried out for a steel coating immersed in a liquid, onto which a spherical wave with an exponential profile is incident.

This paper examines the issue of the effect of a non-stationary wave on a cylindrical cover containing a spring mass. However, a report was eventually made of a steel coating immersed in water that did not maintain a system of discrete masses. The problem was solved in the acoustic setting.

In this work, we study the movement of a rigid spherical insert with a spring mass in a solid elastic medium after the passage of a wave. The problem under consideration is equivalent to the problem of applying an impulse at the beginning of time.

The problem under consideration is an equation of motion for the displacement of an elastic medium in vector form (Lame equations) in the absence of body forces:

$$(\lambda+\mu)\text{grad div}U+\mu\Delta U=\rho\frac{\partial^2 U}{\partial t^2} \quad (1)$$

where are the $\lambda, \mu$ Lamé coefficients, $U$ is the displacement vector, $p$ and is the density of the medium.

If we (1) express the displacement vector as the sum of potential and solenoidal parts,

$$U=\text{grad}\ \varphi+\text{rot}\,\varphi,\quad \text{div}\,\psi=0 \quad (2)$$

Then it follows from equation (1) that the functions $\varphi$ and $\psi$ will satisfy the following wave equations:

$$\Delta^2\varphi-\frac{1}{a^2}\frac{\partial^2\varphi}{\partial t^2}=0 \quad (3)$$

$$\Delta^2\psi-\frac{1}{b^2}\frac{\partial^2\psi}{\partial t^2}=0 \quad (4)$$

$$a=\sqrt{\frac{\lambda+2\mu}{\rho}},\ b=\sqrt{\frac{\mu}{\rho}} \quad (5)$$

The $\varphi$ potential function characterizes longitudinal-compressional waves, $\psi$ the function characterizes transverse (shear) waves, $a$ and $b$ their quantities are the propagation velocities of the corresponding waves.

The strain tensor components are defined as follows:

$$2\varepsilon_{ij}=U_{i,j}+U_{j,i},\quad i=1,2,3. \quad (6)$$

Huq's law is as follows:

$$\sigma_{ij}=\lambda\varepsilon_{ij}\delta_{ij}+2\mu\varepsilon_{ij} \quad (7)$$

where - $\sigma_{ij}$ are the stress tensor components.

$\delta_{ij}$ - is the Chronicler symbol. Since we will use spherical coordinates in the future, let's write these relations in spherical coordinates as well.

Since the problem under consideration is axisymmetric, the displacement vector components and stress components, in spherical coordinates $\varphi$ and $\psi$ wave potentials, are expressed as follows:

$$\begin{cases} u=u_r=\dfrac{\partial\varphi}{\partial r}-\dfrac{1}{r\sin\varphi}\dfrac{\partial}{\partial\theta}\left(\sin\theta\dfrac{\partial\psi}{\partial\theta}\right) \\ \vartheta=u_\theta=\dfrac{1}{r}\dfrac{\partial\varphi}{\partial\theta}+\dfrac{1}{r}\dfrac{\partial}{\partial r}\left(r\dfrac{\partial\psi}{\partial\theta}\right) \end{cases} \quad (8)$$

$$\sigma_r=\frac{\lambda}{a^2}\frac{\partial^2\varphi}{\partial t^2}+2\mu\left(\frac{\partial^2\varphi}{\partial r^2}-\frac{3\partial^2\psi}{\partial r^2}-r\frac{\partial^3\psi}{\partial r^3}+\frac{r}{b^2}\frac{\partial^3\psi}{\partial r\partial t^2}+\frac{1}{b^2}\frac{\partial^2\psi}{\partial t^2}\right)$$

$$\sigma_\theta=\frac{\lambda}{a^2}\frac{\partial^2\psi}{\partial t^2}+2\mu\left(\frac{1}{r}\frac{\partial\varphi}{\partial r}+\frac{1}{r^2}\frac{\partial^2\varphi}{\partial\theta^2}-\frac{1}{b^2}\frac{\partial^2\psi}{\partial t^2}+\frac{\partial^2\psi}{\partial r^2}+\frac{2}{r}\frac{\partial\psi}{\partial r}+\frac{2}{r}\frac{\partial^2\psi}{\partial\theta^2}+\frac{\partial^3\psi}{\partial r\partial\theta^2}\right) \quad (9)$$

$$\tau_{r\theta} = 2\mu\left(\frac{1}{r^2}\frac{\partial\psi}{\partial\theta} - \frac{\partial^3\psi}{\partial r^2\partial\theta} + \frac{1}{b^2}\frac{\partial^3\psi}{\partial\theta\partial t^2} - \frac{1}{r^2}\frac{\partial\varphi}{\partial\theta} + \frac{1}{r}\frac{\partial^2\varphi}{\partial r\partial\theta}\right)$$

Equations (3), (4) correspond to the following form in this coordinate system:

$$\frac{1}{r^2}\frac{\partial}{\partial r}\left(r^2\frac{\partial\varphi}{\partial r}\right) + \frac{1}{r^2\sin\theta}\frac{\partial}{\partial\theta}\left(\sin\theta\frac{\partial\varphi}{\partial\theta}\right) = \frac{1}{a^2}\frac{\partial^2\varphi}{\partial t^2} \quad (10)$$

$$\frac{1}{r^2}\frac{\partial}{\partial r}\left(r^2\frac{\partial\psi}{\partial r}\right) + \frac{1}{r^2\sin\theta}\frac{\partial}{\partial\theta}\left(\sin\theta\frac{\partial\psi}{\partial\theta}\right) = \frac{1}{a^2}\frac{\partial^2\psi}{\partial t^2} \quad (11)$$

$\varphi$ and $\psi$ potentials, as well as one-valued determination of displacement vector and stress tensor components, it is necessary to add boundary and initial conditions to equations (10), (11) and relations (8), (9).

It is assumed that the particles of the medium "sticking" to the insert move without being separated from it.

The ambient pressure at the input is determined as follows.

$$P = \int_0^{\pi} 2\pi r\sigma_r r\sin\theta\cos\theta\,d\theta + \int_0^{\pi} 2\pi r\tau_{\theta_r} r\sin\theta\sin\theta\,d\theta = \quad (12)$$

The input acts according to the following law:

$$\begin{cases} M_1\dfrac{dx_1^2}{dt^2} = P + L(x_2 - x_1) \\ M_2\dfrac{d^2x_2}{dt^2} = -L(x_2 - x_1) \end{cases} \quad (13)$$

where $M_1$ - the mass of the insert, $M_2$ - the mass of the spring body, $x_1$ - the displacement of the insert, $x_2$ - the displacement of the spring body, $L$ - the stiffness of the spring, $P$ - the force of the environment on the insert.

This law of motion can be considered as the boundary conditions for the environment.

Since the medium is motionless at the beginning of time, then the appropriate initial conditions will be as follows:

$$\varphi|_{t=0} = \psi|_{t=0}$$

$$\left.\frac{\partial\varphi}{\partial t}\right|_{t=0} = \left.\frac{\partial\psi}{\partial t}\right|_{t=0} = 0 \quad (14)$$

Thus, the boundary and initial conditions in the non-stationary case were completely determined for the considered problem. It is known that in elasticity theory courses there is and is the only solution to the problem with initial and boundary conditions formulated as above.

## Literature

[1] Горшков А.Г., Григомок Э.И. "Нестационарные задачи теории оболочек, погруженных в жидкость" в сб.: Науч.конф. Ин-т Мех. Моск. ун-та. Тезисы докл. М., 1972-15-РЖ. Мех, 1972,

[2] Агаларов Д.Г., Сейфуллаев А.И., Мамедова Г.А. "Движение включения с полпружинной массой в акустической среде". Труды ИММ АН Азерб. 1997. т. XIV. с.204-207.

[3] Амензаде Ю.А. «Теории упругости», - М: Высшая школа, 1976, -272 с.

[4] FS Latifov, FA Seyfullayev Asymptotic analysis of oscillation eigenfrequency of orthotropic cylindrical shells in infinite elastic medium filled with liquid Trans. NAS Acad. Azer. Ser. Phys.-Tech. Math. Sci 24 (1), 227-230,2004

[5] Сейфуллаев Ф.А., Колебания поперечно подкрепленной цилиндрической оболочки с жидкостью в жидкости.Актуальная наука, с.8-18, 2022

Azerbaijan University of Architecture and Construction
ISSN 2706-7726
Engineering Mechanics
Scientific and Technical Journal
E-mail: engineeringmechanics@azmiu.edu.az

| September 2023 | Issue 14 | Volume 6 | Number 2 | Pages 6-9 |
|---|---|---|---|---|

# PULSATING LIQUID FLOW IN A VISCO-ELASTIC TUBE OF A VARIABLE CIRCULAR CROSS SECTION

**E.A. ASLANOV, V.M. MURADOV, Ch. A. YUSİFOV**
e.aslanov@aztu.edu.az, vaqi.muradov@aztu.edu.az, çərkəz.yusifov @aztu.edu.az

**Abstract.** *Flows of liquid in deformable tubes in many cases may be depicted by the equations of hydraulic approximation [1, 2, 3]. The subject of this work is definition and solution of one-dimensional equations for the case of propagations of long stationary waves in ideal incompressible liquid flowing in a semi-infinite tube of variable circular section, the properties of which comply with linear visco-elastic model of Foigt. The pulsating pressure is given on the tube face. The formulated problem is solved by the method of small parameter.*

**Key words:** incompressible liquid, pulsation, visco-elastic tube, stationary waves, heterogeneous equations, semi-infinite.

**1.** Let us develop axisymmetric equations of one-dimensional motion and continuity at laminar flow of ideal incompressible liquid in a linear visco-elastic thin tube of variable circular section. Considering slow flow, then the equation of liquid flow along axis *x* will be as follows:

$$\frac{\partial p}{\partial x} = -\rho \frac{\partial u}{\partial t} \qquad (1.1)$$

Where $p(x,t)$ - pressure, $\rho$ - density of liquid, $u(x,t)$ - its axial velocity. Considering the property of equality of hydrodynamic and hydrostatic pressures at passage of long waves, we assume:

$$p = \sigma k(x), \quad k = hR^{1-}(x); \qquad (1.2)$$

Here $\sigma$ - hoop stress, *h* = const - tube thickness, *R(x)* - its radius.
Taking the law of deformation in the form of $\sigma = Ee + \mu\dot{e}$, we write expression (1.2) as follows:

$$p = k(x)\left[Ee + \mu\dot{e}\right] \qquad (1.3)$$

Where *E* and $\mu$ - correspondingly the module of elasticity and viscosity coefficient of the tube, $e = \bar{\omega}R^{-1}(x)$ - hoop strain, $\bar{\omega}(x,t)$ - radial displacement. The point above *e* means differentiation with time *t*. Inserting a dimensionless magnitude $\bar{\omega} = \bar{\omega}h^{-1}$, the formula (1.3) takes the appearance: $p = \left[E\omega + \mu\dot{\omega}\right]k^2(x)$ and equation of movement (1.1) to be re-written as follows:

$$\frac{\partial}{\partial x}\left\{k^2(x)\left[Ew + \mu\dot{w}\right]\right\} = -\rho\frac{\partial u}{\partial t} \qquad (1.4)$$

The equation of continuity for the deformed tube of variable section will take the appearance:

$$\frac{\partial}{\partial x}(uF)+L\frac{\partial \overline{w}}{\partial t}=0, \quad F=\pi R^2(x), \quad L=2\pi R(x). \tag{1.5}$$

The last member in the equation (1.5) is a consequence of impermeability condition and it characterizes the consumption of liquid due to deformation of tube walls. Considering abovementioned indications, the continuity equation (1.5) takes finally the form.

$$\frac{\partial w}{\partial t}=-\frac{1}{2}k(x)\frac{\partial}{\partial x}\left[k^{-2}(x)u\right] \tag{1.6}$$

Cancelling out through differentiation the velocity $u$ from the equations (1.4) and (1.6), we approach to the equation for definition of $w$.

$$\rho^{-1}k^{-2}x'\frac{\partial}{\partial x}\left\{k^2\left[Ew+\mu\dot{w}\right]\right\}-\frac{1}{2}\rho^{-1}k^{-1}\frac{\partial^2}{\partial x^2}\left\{k^2\left[Ew+\mu\dot{w}\right]\right\}=-\frac{\partial^2 w}{\partial t^2} \tag{1.7}$$

Because of presence in the equation (1.7) of variable coefficients, its precise solution is quite difficult. For the approximate solution we use the method of small parameter.

**2.** Let's consider a case of semi-infinite tube, when on its face we have the pulsating pressure of the Following appearance:

$$p(0,t)=\overline{p}_0\exp(i\omega t) \tag{2.1}$$

where $\omega$ - a given circular frequency, and $\overline{p}_0$ - a given empirical pressure. Let's represent *R(x)* as $R(x)=R_0\left[1+\varepsilon\lambda(x)\right]$, where $\varepsilon<<1$ - small parameter, and $\lambda(x)$ - a given function, characterizing a form of perturbation of tube radius. It is natural to assume that $\lambda(x)$ has limited continuous derivatives up to the second order. Then we choose such an $\varepsilon$, that *k(x)* approximately may take the following form:

$$k(x)\sim hR_0^{-1}\left[1-\varepsilon\lambda(x)\right] \tag{2.2}$$

Considering the last relation and inserting indications $c_0^2=1/2hR_0^{-1}E\rho^{-1}$ and $c_1^2=1/2hR_0^{-1}\mu\rho^{-1}$, , the equation (1.7) to have the following appearance:

$$\begin{aligned}&\frac{\partial^2 w}{\partial t^2}-c_0^2\frac{\partial^2 w}{\partial x^2}-c_1^2\frac{\partial^3 w}{\partial x^2\partial t}+\varepsilon\left\{c_1^2\lambda(x)\frac{\partial^3 w}{\partial x^2\partial t}+c_0^2\lambda(x)\frac{\partial^2 w}{\partial x^2}+\right.\\&+2c_1^2\lambda'(x)\frac{\partial^2 w}{\partial x\partial t}+2c_0^2\lambda'(x)\frac{\partial w}{\partial x}+2\left[\varepsilon\left(1+\varepsilon\lambda(x)\right)\lambda'^2(x)+\lambda''(x)\right]c_1^2\frac{\partial w}{\partial t}+\\&\left.2\left[\varepsilon\left(1+\varepsilon\lambda(x)\right)\lambda'^2(x)+\lambda''(x)\right]c_0^2 w\right\}=0\end{aligned} \tag{2.3}$$

Let's put into the expression for the pressure *p* and in the equations (1.4) and (2.3) the following:

$w=w_0+\varepsilon w_1+...,\qquad p=p_0+\varepsilon p_1+...,\qquad u=u_0+\varepsilon u_1+...$

Let's consider that the order of unknown functions does not increase ar their differentiation along each of the variables. Then, having equalized coefficients at equal powers $\varepsilon$, we get a zero and first approximation for the unknown functions:

$$\frac{\partial^2 w_0}{\partial t^2}-c_1^2\frac{\partial^3 w_0}{\partial x^2\partial t}-c_0^2\frac{\partial^2 w_0}{\partial x^2} \tag{2.4}$$

$$\begin{aligned}&\frac{\partial^2 w_1}{\partial t^2}-c_1^2\frac{\partial^3 w_1}{\partial x^2\partial t}-c_0^2\frac{\partial^2 w_1}{\partial x^2}=-\left\{c_1^2\lambda(x)\frac{\partial^3 w}{\partial x^2\partial t}+c_0^2\lambda(x)\frac{\partial^2 w_0}{\partial x^2}+2c_1^2\lambda'(x)\frac{\partial^2 w_0}{\partial x\partial t}+\right.\\&\left.+2c_0^2\lambda'(x)\frac{\partial w_0}{\partial x}+2c_1^2\lambda''(x)\frac{\partial w_0}{\partial t}+2c_0^2\lambda''(x)w_0\right\}\end{aligned} \tag{2.5}$$

$$p_0 = h^2 R_0^{-2} \left\{ E w_0 + \mu \frac{\partial w_0}{\partial t} \right\} \tag{2.6}$$

$$p_1 = h^2 R_0^{-2} \left\{ E w_1 + \mu \frac{\partial w_1}{\partial t} \right\} - 2h^2 R_0^{-2} \lambda(x) \left\{ E w_0 + \mu \frac{\partial w_0}{\partial t} \right\} \tag{2.7}$$

$$h^2 R_0^{-2} \frac{\partial}{\partial x} \left\{ E w_0 + \mu \frac{\partial w_0}{\partial t} \right\} = -\rho \frac{\partial u_0}{\partial t} \tag{2.8}$$

$$h^2 R_0^{-2} \frac{\partial}{\partial x} \left\{ \left[ E w_1 + \mu \frac{\partial w_1}{\partial t} \right] - 2\lambda(x) \left[ E w_0 + \mu \frac{\partial w_0}{\partial t} \right] \right\} = -\rho \frac{\partial u_1}{\partial t} \tag{2.9}$$

It is not hard to show that the solution of the zeroth approximation, considering its limitation at $x \to \infty$, has the appearance:

$$w_0 = \alpha_0 \exp\left[ i(\omega t + \gamma x) \right] \tag{2.10}$$

$$p_0 = \alpha_0 \xi \exp\left[ i(\omega t + \gamma x) \right] \tag{2.11}$$

$$u_0 = \alpha_0 \eta \exp\left[ i(\omega t + \gamma x) \right] \tag{2.12}$$

where $\alpha_0$ - constant of integration>

$$\xi = h^2 R_0^{-2} (E + i\omega\mu), \qquad \eta = h^2 R_0^{-2} i(Ei - \omega\mu) \gamma \omega^{-1} \rho^{-1}$$

The value $\gamma$ to be defined from the disperse equation reducing to as follows:

$$\gamma^2 = \omega^2 \Big/ \left( c_0^2 + i\omega c_1^2 \right), \tag{2.13}$$

and when writing (2.10) - (2.12) it was assumed that $\operatorname{Re}\gamma < 0$.

It is easy to determine that the solution of the disperse equation has the following quality:

$\gamma_1 = \operatorname{Re}\gamma - i m_\gamma$, $\gamma_2 = -\operatorname{Re}\gamma + i m_\gamma$. Therefore due to limitation of the unknown solution we use a second root.

**3.** The first approximation. Considering (2.10) into equation (2.) we have the following:

$$\frac{\partial^2 w_1}{\partial t^2} - c_1^2 \frac{\partial^2 w_1}{\partial x^2 \partial t} - c_0^2 \frac{\partial^2 w_1}{\partial x^2} = -\alpha_0 f(x) \exp(i\omega t) \tag{3.1}$$

where for short writing we have the following indication:

$$f(x) = \left\{ -c_1^2 i\omega\gamma^2 \lambda(x) - c_0^2 \gamma^2 \lambda(x) - 2c_1^2 \gamma\omega\lambda'(x) + 2c_0^2 i\gamma\lambda'(x) + 2c_1^2 i\omega\lambda''(x) + 2c_0^2 \lambda''(x) \right\} e^{i\gamma x} \tag{3.2}$$

It is obvious, that *f(x)* - limited function. Let put $w_1(x,t) = y(x)\exp(i\omega t)$, into equation (3.1) and re-write it to get:

$$y'' + \gamma^2 y = \alpha_0 \omega^{-2} f(x) \tag{3.3}$$

The common solution of heterogeneous equation (3.3) due to its limitation along infinity has the following appearance:

$$y(x) = \frac{\alpha_0 \omega^{-2}}{2i\gamma} e^{-i\gamma x} \int_x^\infty e^{i\gamma\tau} f(\tau) d\tau + \frac{\alpha_0 \omega^{-2}}{2i\gamma} e^{i\gamma x} \int_0^x e^{-i\gamma\tau} f(\tau) d\tau + C_2 e^{i\gamma x}. \tag{3.4}$$

So, the function *y(x)* is defined with the precision up to constants $\alpha_0$ and $C_2$. In order to determine them, let's use the condition (2.1). Then $\alpha_0 = \xi^{-1} p_0$, $y(0) = 2\alpha_0 \lambda(0)$ and finally we have:

$$w = (\xi^{-1}\overline{p}_0 e^{i\gamma x} + \varepsilon y(x))\exp(i\omega t),$$

$$p = \left(\overline{p}_0 e^{i\gamma x} + \varepsilon\left[\xi y(x) - 2\overline{p}_0\lambda(x)e^{i\gamma x}\right]\right)\exp(i\omega t),$$

$$u = (\eta\xi^{-1}\overline{p}_0 e^{i\gamma x} + \varepsilon\left[i\xi(\rho\omega)^{-1}y'(x) - 2\xi\eta\overline{p}_0\lambda(x)e^{i\gamma x} - 2i(\rho\omega)^{-1}\overline{p}_0\lambda'(x)e^{i\gamma x}\right]\exp(i\omega t),$$

where

$$y(x) = \frac{\xi^{-1}\overline{p}_0\omega^{-2}}{2i\gamma}\left(e^{-i\gamma x}\int_x^\infty e^{i\gamma\tau}f(\tau)d\tau + e^{i\gamma x}\int_0^\infty e^{-i\gamma\tau}f(\tau)d\tau\right) + \xi^{-1}\overline{p}_0\left(2\lambda(0) - \frac{\omega^{-2}}{2i\gamma}\int_0^\infty e^{i\gamma\tau}f(\tau)d\tau\right)e^{i\gamma x}.$$

It should be mentioned that acquisition of further approximations does not represent difficulties of principle, as in this case this would bring to the solution of heterogeneous equations of (3.3), but with a bigger expression for the function *f(x)*. Herewith a physical value is represented through real part of the constructed solution.

## References


1. Reuderink P.J., Hoogstraten H.W., Sipkema P. , Hillen B., Westerhof N. Linear and nonlinear one-dimensional model of pulse wave transmission at high Womersley numbers, J. Biomech., 22 (8/9), pp.819-827, 1989.
2. Regirov S.A Rutkevich N.M. In a coll. Several questions of mechanics of continuous medium, Publish. of Moscow State University, 1978.
3. Sedov. L.I .Continuum Mechanics. Publish. "Nauka", Vol.2, Moscow, 1970.
4. Marchenko V.A. Spectral theory of Sturm–Liouville operators. Publish. "Naukova dumka", Kiev, 1972.
5. Aslanov E.A. A problem of wave propagation in an elastic tube containing heterogeneous liquid. ISSN 2519-8742. Mechanics. Researches and innovations. Vol.13. Gomel, 2020.

Azerbaijan University of Architecture and Construction
ISSN 2706-7726
Engineering Mechanics
Scientific and Technical Journal
E-mail: engineeringmechanics@azmiu.edu.az

| September 2023 | Issue 14 | Volume 6 | Number 2 | Pages 10-12 |
|---|---|---|---|---|

# REASONS FOR FAILURE OF HYDRAULIC SYSTEMS OF TECHNOLOGICAL MACHINES AND WAYS TO IMPROVE THEIR PERFORMANCE

**A.T.MEHRALIYEV, G.V.NOVRUZOVA**
*Azerbaijan University of Architecture and Construction*
alif.mehraliyev@gmail.com , gulnarnovruzova74@mail.ru

***Abstract:*** *The presented article discusses the causes of failures and decreased performance in the hydraulic systems of technological machines. İt is acknowledged that the reliability of machines is connected with friction and wear of contact surfaces. On the other hand, the cause of defects is contamination of the working fluid substances with mechanical particles. In order to detect changes in oil quality and possible contamination in a timely manner, it is necessary to carry out systematic oil monitoring.*

**Key words:** hydraulic system, working liquid, failure, wear, analysis, express analyzer

Increasing the level of mechanization and automation of road construction works, performed mainly with the use of complex machines, requires not only quantitative and qualitative growth of the fleet of machines, but also ensuring the reliability of their functioning. Recently, there are quite range of manufactured technological machine. The main types of manufactured equipment include various excavators, scrapers, bulldozers, rollers, motor graders and others.

In the construction of technological machines, hydraulic drive and various hydraulic systems is of great importance. Hydraulic systems and hydraulic drives are widely used as executive bodies of control systems and automation of processes, following drives of steering systems, drives of working bodies. Modern trends in the production and operation of technological machines and equipment in mechanical engineering is the improvement of its qualitative and quantitative indicators. Increasing one of the main quality indicators of machine durability is equivalent not only to increasing productivity, but also to the release of significant resources, economy of raw materials, other materials and energy. The problem of the durability of machines is directly connected to the issues of friction and wear of the mating surfaces of the parts odies of machines.

Analysis of failures of hydraulic systems of technological machines allowed to identify the causes of loss of performance of individual units. For example, in axial-piston pumps and hydraulic engines, failure occurs as a result of wear of the spherical surface and curvature of connecting rods, wear of end surfaces, piston holes and seats in the block, wear of shaft necks, wear of pistons. İn gear pumps as a result of wear of the inner surface and seats of the body and covers, wear of bushings; in vane pumps because of wear of the end surfaces of stators and discs, wear of blades, pins, ends and grooves in rotors. The most worn places in hydraulic cylinders include the inner and end surface of the cylinder body, the ends and landing surfaces of the covers. The landing surface of the guide bushings, the outer surface of the plungers and pistons, the threaded connections and seals. It can be seen that the problem of the durability of machines is directly related to the issues of friction and wear of the mating surfaces of the parts. The experience of operating hydraulic systems shows that about 30% of all failures are due to malfunctions of precision pairs that perform the functions of regulators, distributors, and displacement elements. Practically, on the details of each

precision pair of hydraulic aggregator, which have normally worked out the warranty resource, when examining the technical condition, various damages to the working surfaces are revealed, which manifest themselves most often in the form of scratches.

In addition to the specified types of damage, in the drives of technological machines and a significant proportion of the machines are failures caused by contamination of the working fluid with mechanical particles during the production and installation of the drive, as well as during refueling. During the operation of the drive, the wear products of the mating parts continuously flow into the liquid. During collecting, polluting substances are released during oxidizing processes between liquids and additives used to improve the operational properties of the working fluid. When the working fluid is contaminated, the wear of the distribution devices of the pumps is intensively observed, which the volumetric efficiency decreases is consequently. When the liquid moves at a high speed, the contamination in the form of solid particles acts on the surface of the parts like an abrasive emulsion. With the passage of time, the gaps increase, the overlaps decrease, and the flow rates of the throttles and nozzles change. When fluid leaks increase due to wear of drive elements, system rigidity and speed of movement of executive bodies decrease. As a result, the oil ages, and its operational properties deteriorate.

A methodology for increasing the efficiency and performance of technological machines during their technical operation in production has been developed. For the systems of technical service and repair of machines are analyzed. Systems of scheduled notification, firm and technical maintenance are used to carry out process on technical maintenance. Repair of technological machines and preventive measures are applied in case of accidents and failures. It can be noted that the most promising direction of carrying out technical maintenance and repair, increasing the efficiency of the machine, controlling the operational properties of working liquids is conducting a preventive analysis. It should be noted that in developed countries today oil analysis is the main method for diagnosing the technical condition of machine equipment. In addition, the diagnosis of the oil working in the mechanism is characterized by the following advantages: it is not necessary to stop the operation of the machine; no need for disassembly; the possibility of changing the oil according to its actual performance, and not according to mileage; low labor intensity of diagnostics and analysis.

Oil that has lost its protective properties before time can increase the rate of wear of hydraulic drive elements several times and lead to its eventual breakdown. In order to detect changes in the quality of oil and possible contamination in time, it is necessary to carry out a systematic control of the oil. Checking the liquid sample can be carried out by the following methods:

1. Weighing control (GOST 6370-83 and ISO 4405);
2. optical-microscopic control (ISO 4407);
3. with the help of an express analyzer or an automatic particle counter;
4. Chemical control composition of the mixture.

Currently, express analysis is considered the most promising method at enterprises engaged in the operation of technological machines and equipment. To check the contamination of the working fluid, an express-analyzer is used with a special stand. To determine the composition of particles of polluting substances, waste oil, taken as a sample, is poured into each glass of the express-analyzer and rotated at the same speed. The mass concentration of particles of polluting substances, collected under the action of centrifugal force, and the volume of sediment are determined. Concentrated liquids of the same mass may contain particles of different quantities and sizes. After determining the specific weight of the pollutant, the amount of particles is determined. The composition of particles is checked with the help of a microscope. The responsible person notify the possible problems, and he examines the change in the condition of each working element of the machine during a certain time and sends the machine to production or repair. Hence, it is clear that the analysis of the working fluid with an express analyzer is more promising, since it reveals possible malfunctions in the devices of the hydraulic system. It can be noted that the most promising direction in carrying out technical maintenance and repair, increasing the efficiency of

working with the machine, controlling the operational properties of working fluids is conducting a preventive analysis.

**Conclusion:** Improving the technical operation system is an important question for maintaining the efficiency of technological machines during operation. According to the results of the conducted studies, the most promising direction of performing technical service and repair work, increasing the efficiency of the machine and maintaining operational properties under control is conducting a preventive analysis.

**Literature**

1. Sharifov. A.R., Mehraliyev. A.T., Talibov T.A. Control of contamination of working fluids of hydraulic systems of technological machines// AzMIU, Scientific Works, Baku. 2019. No. 1. p. 216-220

2. Karlyushenko, A.A. Filtration of working liquid hydrosystem // A.A Karlyushenko // Building technology and technologies. 2008 No. 3 pp. 162-168

Azerbaijan University of Architecture and Construction
ISSN 2706-7726
Engineering Mechanics
Scientific and Technical Journal
E-mail: engineeringmechanics@azmiu.edu.az

| September 2023 | Issue 14 | Volume 6 | Number 2 | Pages 13-19 |
|---|---|---|---|---|

# A PROBLEM OF WAVE PROPAGATION IN AN ELASTIC TUBE CONTAINING HETEROGENEOUS LIQUID.

**E.A. ASLANOV, V.M. MURADOV, Ch. A. YUSİFOV**
e.aslanov@aztu.edu.az, vaqi.muradov@aztu.edu.az, çərkəz.yusifov @aztu.edu.az

**Abstract.** *This work explores solution of a one-dimensional problem about propagation of harmonic waves in an orthotropic elastic tube containing heterogeneous incompressible liquid, rheological behaviour of which is described by Maxwell model.*
Numerically depicted an influence of concentration of inclusions onto wave characteristics for the case of propagations of long stationary waves in heterogeneous liquid flowing in an elastic tube of variable circular section, the properties of which comply with linear visco-elastic model of Foigt. The solution of this problem is defined by singular boundary problem of Sturm–Liouville.
It is assumed that the tube is rigidly fixed to surrounding and, thus, its longitudinal displacement is equal to null. Cases of finite and semi-infinite tubes are considered.
**Keywords:** Wave propagation, elastic tube, heterogeneous liquid, harmonic waves, viscoelasticity, haemodynamics.

## 1. Introduction

One of the specific features of heterogeneous bodies is their elastic characteristics that are continuous functions of coordinates and that, as a matter of rule, have a required number of derivatives.
The flow of liquid in deformed tubes in many cases can be defined through equations of hydraulic approximation. The majority of works in this direction are based on the assumption of homogeneity of tube material. In many practically important cases we have to deal with propagation of stationary waves in elastic tubes that contain heterogeneous liquids and in which velocity of propagation is a wave local parameter and it is considered as a function of coordinates.
By study of flow of colloidal solutions, suspensions, high-molecular compounds we use rheological models representing different combinations of elastic and viscous elements. Their behaviour at least qualitatively corresponds to the behaviour of abovementioned mediums.
Theoretical developments, obtained at solutions of problems of interaction of a cylindrical shell with a viscous liquid flowing in it in force of definite physical approximations may be carried over to the case of disperse liquid. This generalization is made through introduction of an effective coefficient of dynamic viscosity.
From the qualitative analysis it follows that at known boundary conditions (functional systems) rheological properties of a liquid have an apparent impact on its velocity and hydraulic impedance, and viscosity of tube material on displacement, velocity and impedance.
It should be noted that due to linearity of the problem the real parts of solutions, obtained from the arbitrary kernels of heredity, to have their physical meaning.

## 2. Mathematical formulation

Before all, let's define the system that describes propagation of waves of small amplitude in a suspension flowing in a deformed shell. First let's give a mathematical model of a liquid. It can be

considered [1] that multiphase systems represent mixtures of hard particles, liquefied droplets and bubbles (discrete phases) that are widespread in a liquid (carrying and continuous phase).
Research of dynamics of multiphase systems grasps wide fields of science and technology and is connected with a lot of fundamental problems. Here, we can mention, e.g. such important cases as pumping-over of cryogenic liquids, radioactive precipitation, deposition, haemodynamics etc. for our purposes we will interpret disperse medium as incompressible Newtonian liquid with the density of water $\rho_f$, in which there are non-interacting particles of identical size. It is assumed that the velocities of continuous and discrete phases are the same. Then, an effective dynamic viscosity $\mu$ of diluted suspension of hard spherical particles having neutral buoyancy (i.e. non-depositing and non-emerging) in a liquid carry-over with a viscosity of $\mu_0$can be calculated through the formula of Einstein [2].

$$\mu = \mu_0\left(1+\frac{5}{2}\phi\right) \qquad (2.1)$$

where $\phi$ - volumetric concentration of particles in parts of units. This result was generalized by Taylor [2] on suspension of droplets which keep their spherical form, e.g. due to surface tension. A consecutive correlation is as follows:

$$\mu = \mu_0\left\{1+\phi\left(\frac{\mu_0+\frac{5}{2}\bar{\mu}}{\mu_0+\bar{\mu}}\right)\right\} \qquad (2.2)$$

in which $\bar{\mu}$ - viscosity of liquid that makes droplets. When $\bar{\mu}$ becomes infinitely large, i.e. when the droplets appear to become, actually, hard particles, this correlation is reduced to (2.1).
Effective viscosity of suspension of hard asymmetric particles increases as with growth of particles concentration as well as with power of their asymmetry. This dependence is defined by the expression:

$$\mu = \mu_0(1+K\phi)$$

where *K* (factor of geometry) more than 5/2. In case of hard mixtures of non-spherical particles having the form of ellipsoids of rotation in relation to half-axles 6:1, *K* to take the value equal to 5 and viscosity of mixture to increase as follows [2]:

$$\mu = \mu_0(1+5\phi) \qquad (2.3)$$

The assumptions made give opportunity to consider the known contact conditions of conjugation of linear hydroelasticity. If now to take into consideration the condition of impermeability and assume that the tube is rigidly fixed to surroundings, as a result of which the wall material cannot make any movement along its axis *x*, then based on abovementioned assumptions mean equations of impermeability and those of Navier–Stokes for the mixture as a whole can be written in the following form [3]:

$$\frac{\partial u}{\partial x}+\frac{2}{R}\frac{\partial w}{\partial t}=0 \qquad (2.4)$$

$$\frac{1}{\rho_f}\frac{\partial p}{\partial x}+\frac{\partial u}{\partial t}+\frac{8\mu}{\rho_f R^2}u=0 \qquad (2.5)$$

In (2.4)-(2.5) *w(x,t)* - is a radial displacement of a tube of radius *R* and thickness *h*, *u(x,t)* - is a mean velocity of mixture flow, *p(x,t)* - hydrodynamic pressure. As for the dynamic coefficient of viscosity of mixture$\mu$, then it, depending on concentration $\phi$, must be defined in actual examples through formula (2.1) -(2.3)
The system (2.4) and (2.5) can be reduced to a single equation of the following form:

$$\frac{1}{\rho_f}\frac{\partial^2 p}{\partial x^2}+\frac{8\mu}{\rho_f R^2}\frac{\partial u}{\partial x}-\frac{2}{R}\frac{\partial^2 w}{\partial t^2}=0$$

Substituting here $\frac{\partial u}{\partial x}$ for $\frac{2}{R}\frac{\partial w}{\partial t}$and putting this into the last dependence, we have:

$$\frac{1}{\rho_f}\frac{\partial^2 p}{\partial x^2} - \frac{16\mu}{\rho_f R^3}\frac{\partial w}{\partial t} - \frac{2}{R}\frac{\partial^2 w}{\partial t^2} = 0 \qquad (2.6)$$

Next, for completion of equation (2.6), let's write down the equation of condition for the tube material, considering that it is elastic, orthotropic and thin-walled. For these conditions it is sufficient to use the following correlation [4]:

$$p = \frac{E_2}{1-v_1 v_2}\frac{h}{R^2}w + \rho_* h\frac{\partial^2 w}{\partial t^2} \qquad (2.7)$$

Here, $\rho_*$ - is a density of tube material, $v_1$and $v_2$- are coefficients of Poisson, $E_2$ - modulus of elasticity in a circular direction. It should be mentioned that the condition of Maxwell to hold herewith:

$$E_2 v_1 = E_1 v_2$$

where $E_1$ - is an axial Young's modulus.

Let's take in the equation (2.7) the second derivative along $x$ and consider the result in (2.6). Then, moving to next indications

$$c_0^2 = \frac{E_2}{2\rho_f(1-v_1 v_2)}\frac{h}{R} \text{ and } \frac{\rho_*}{\rho_f} = \rho$$

we get the following equation

$$\frac{\partial^2 w}{\partial x^2} + \rho\frac{Rh}{2c_0^2}\frac{\partial^4 w}{\partial x^2 \partial t^2} - \frac{8\mu}{\rho_f c_0^2 R^2}\frac{\partial w}{\partial t} - \frac{1}{c_0^2}\frac{\partial^2 w}{\partial t^2} = 0 \qquad (2.8)$$

which describes dynamic behaviour of the system "shell-liquid".

**3. Numerical method and parameters**

For description of complex impulses, typical for wave processes, we consider the method of Fourier; hence solution of equation (2.8) to be represented in from of final sum of the main oscillation and higher harmonics. [5] This statement enables to represent the function $w$ in the following form:

$$w = \sum_{s=1}^{s} y_s(x)\, exp(is\omega t) \qquad (3.1)$$

Here, $y_s(x)$ - unknown complex functions of coordinates of dimension,

$\omega$ - known angular frequency, $i$ - imaginary unit, and $S$ - harmonic value.

In force of linearity of the system let's follow the passage of each harmonics $s$ and then for definition of the form of disturbance let's sum each component related to the given point. Substituting (3.1) into (2.8), for $s_{th}$ harmonics we have:

$$y_s'' + \lambda_s^2 y_s = 0 \qquad (3.2)$$

where the prime means differentiation along coordinate $x$, and value $\lambda_s$is defined from the solution of the following disperse equation:

$$\lambda_s^2 = \frac{\frac{\omega}{c_0^2}s\left\{\omega s - i\frac{8\mu}{\rho_f R^2}\right\}}{1-\rho\frac{Rh}{2c_0^2}\omega^2 c_0^2} \qquad (3.3)$$

Dividing equation (3.3) into real and imaginary parts and introducing the following indications

$$\lambda_{0s} = \frac{\frac{s^2\omega^2}{c_0^2}}{1-\rho\frac{Rh}{2c_0^2}\omega^2 s^2}, \qquad \lambda_{1s} = \frac{\frac{s^2\omega^2}{c_0^2}\frac{8\mu}{\rho_f R^2}}{1-\rho\frac{Rh}{2c_0^2}\omega^2 s^2}$$

we get

$$\lambda_s^2 = \lambda_{0s} - i\lambda_{1s} \qquad (3.4)$$

Solving disperse equation (3.4), and choosing the root Im$\lambda < 0$, for$\lambda_s$through the known formula of calculation of square root from a complex value, we find:

$$\lambda_s = \delta_{0s} - i\delta_{1s} \qquad (3.5)$$

In (3.5) it is assumed that

$$\delta_{0s} = \left\{\frac{1}{2}(\lambda_{0s} + m)\right\}^{\frac{1}{2}}, \quad \delta_{1s} = \left\{\frac{1}{2}(m_s - \lambda_{0s})\right\}^{\frac{1}{2}}, \text{ and } m_s = (\lambda_{0s}^2 + \lambda_{1s}^2)^{\frac{1}{2}}$$

With this the velocity of propagation of $s_{th}$ wave is defined as $\frac{s\omega}{\delta_{0s}}$, and $\delta_{1s}$ - damping coefficient.

**4. Derivations and numerical analysis**

It should be mentioned first that the common solution to the equation (3.2) is written in the form:

$$y_s - A_s e^{-i\lambda_s x} + B_s e^{i\lambda_s x} \qquad (4.1)$$

where $A_s$ and $B_s$ - constants of integration determined from the boundary conditions to be defined further. Now for function *w* and *p* we may write:

$$w = \sum_{s=1}^{S}\left\{A_s e^{-i\lambda_s x} + B_s e^{i\lambda_s x}\right\} exp(is\omega t) \qquad (4.2)$$

And

$$p = \left\{\frac{E_2}{1-\nu_1\nu_2}\frac{h}{R^2} - \rho_* h\omega^2\right\}\sum_{s=1}^{S}\left\{A_s e^{-i\lambda_s x} + B_s e^{i\lambda_s x}\right\} exp(is\omega t) \qquad (4.3)$$

Both of these results can be derived from formulas (2.7) and (3.1), in case we consider in them the dependence (4.1).

Now it is remained to define the velocity of liquid flow. For this we state:

$$u = \sum_{s=1}^{S} U_s(x)\, exp(is\omega t) \qquad (4.4)$$

With this in mind and using the equation (2.5), after elementary conversions it is possible to find:

$$u = -i\left\{\frac{E_2}{1-\nu_1\nu_2}\frac{h}{R^2} - \rho_* h\omega^2\right\}\sum_{s=1}^{S}\frac{\lambda s}{I_s}\left(-A_s e^{-i\lambda_s x} + B_s e^{i\lambda_s x}\right) exp(is\omega t) \qquad (4.5)$$

where the value

$$I_s = \rho_f\left(is\omega + \frac{8\mu}{\rho_f R^2}\right),$$

that is defined as

$$I_s = \frac{-\left(\frac{\partial p_s}{\partial x}\right)}{u_s}$$

is a hydraulic impedance of $s_{th}$ harmonic. The value of $\frac{8\mu}{R^2}$characterizes hydraulic resistance, and $\omega s\rho_f$- induction. Hence it follows that hydraulic resistance linearly depends on $\mu$, and induction - on harmonic *s*.

Now, let's describe propagation of pressure, velocity of flow and displacement for a straight tube of length *l*. For this let's formulate the following boundary conditions. Let's pressure changes with the law

$$\sum_{s=1}^{S} p_{0s}\, exp(is\omega t) \qquad (4.6)$$

at $x=0$ and for simplicity it equals to zero at $x=l$. In (4.6) $p_{0s}$- are known empirical constants. In force of written boundary conditions, let's write an obtained system of algebraic equations necessary for definitions of $A_s$ and $B_s$. It has the following form:

$\alpha(A_s + B_s) = p_{0s}$,

$A_s e^{-i\lambda_s l} + B_s e^{i\lambda_s l} = 0$

$\alpha = \dfrac{E_2}{1 - v_1 v_2}\dfrac{h}{R^2} - \rho_* h\omega^2$

Hence it follows that

$$A_s = -i\frac{p_{0s}e^{i\lambda_s l}}{2\alpha \sin\lambda_s l}, \text{ and } B_s = i\frac{p_{0s}e^{-i\lambda_s l}}{2\alpha \sin\lambda_s l}$$

Using these equations in (4.2), (4.3) and (4.5), we find:

$$w(x,t) = -\frac{1}{\alpha}\sum_{s=1}^{S} p_{0s}\frac{\sin\lambda_s(x-l)}{\sin\lambda_s l}exp(is\omega t) \quad (4.7)$$

$$p(x,t) = -\sum_{s=1}^{S} p_{0s}\frac{\sin\lambda_s(x-l)}{\sin\lambda_s l}exp(is\omega t) \quad (4.8)$$

$$u(x,t) = \sum_{s=1}^{S}\frac{\lambda_s}{I_s}p_{0s}\frac{\cos\lambda_s(x-l)}{\sin\lambda_s l}exp(is\omega t) \quad (4.9)$$

Consecutive correlations for the limited case of semi-infinite tube can be obtained through calculation of limit of the expressions (4.7)-(4.9) at $l$ approaching infinity. It may be shown that at $\mathrm{Im}\lambda_s < 0$ (that was mentioned earlier) and:

$$\lim_{l\to\infty}\frac{\sin\lambda_s(x-l)}{\sin\lambda_s l} = -e^{-i\lambda_s x}$$

$$\lim_{l\to\infty}\frac{\cos\lambda_s(x-l)}{\sin\lambda_s l} = -ie^{-i\lambda_s x}$$

then from the abovementioned formulas it follows that the related solution can be written as follows:

$$w(x,t) = \frac{1}{\alpha}\sum_{s=1}^{S} p_{0s}e^{-i\lambda_s x}exp(is\omega t) \quad (4.10)$$

$$p(x,t) = \sum_{s=1}^{S} p_{0s}e^{-i\lambda_s x}exp(is\omega t) \quad (4.11)$$

$$u(x,t) = i\sum_{s=1}^{S}\frac{\lambda_s}{I_s}p_{0s}e^{-i\lambda_s x}exp(is\omega t) \quad (4.12)$$

It should be noted that in force of the system linearity, the physical meaning has the true parts of the built solution.

Let's move forward to calculation of the amplitude of pressure $|p_s|$ for the $s_{th}$ harmonic. We have:

$p_s = p_{0s}e^{-i\lambda_s x}e^{is\omega t}$

hence, taking into account (3.5) and considering Euler's formula we may write:

$p_s = p_{0s}e^{-i\delta_{0s}x}e^{-\delta_{1s}x}\{cos(s\omega t) + i\,sin(s\omega t)\}$

From the previous equation it is easy to get for pressure amplitude that:

$$|p_s| = p_{0s}e^{-\delta_{1s}x} \quad (4.13)$$

Following the equation (4.10) for the amplitude of displacement we may write:

$$|w_s| = \frac{p_{0s}}{\alpha}e^{-\delta_{1s}x} \quad (4.14)$$

Doing the same we can calculate the amplitude of flow velocity, that for the $s_{th}$ harmonic has the following appearance:

$$|u_s| = p_{0s}e^{-\delta_{1s}x}\frac{\sqrt{a_{1s}+a_{2s}}}{a_{0s}} \quad (4.15)$$

Here the coefficients $a_{0s}, a_{1s}$ and $a_{2s}$ to be written down as follows:

$$\alpha_{0s} = \frac{64\mu^2}{R^4} + \rho_f^2 s^2\omega^2,\ \alpha_{1s} = \frac{8\mu}{R^2}\delta_{1s} + \rho_f s\omega\delta_{0s},\ \alpha_{2s} = \frac{8\mu}{R^2}\delta_{0s} - \rho_f s\omega\delta_{1s}$$

**4. Results and Conclusions**

For estimation of the result, received form considering an "amendment" to the dynamic viscosity coefficient, we are interested to see the influence of heterogeneity. In order to get a numerical result, we assume that the tube is orthotropic. The numerical experiment with the following system parameters is proposed:

$R = 0.5cm; \bar{\mu} = 0.1g/cm \cdot sec;$
$h = 0.2cm; \rho_f = \rho_* = 1g/cm^3; \rho = 1;$
$\omega = 2\pi\, sec^{-1}; x = 0; E_2 = 4 \cdot 10^6 dyn/cm^2, v_1 = 0.1, v_2 = 0.3,$
$p_{01} = 1.4 \cdot 10^3 dyn/cm^2, p_{03} = 2.4 \cdot 10^2 dyn/cm^2.$

Table 1 shows the values of wave velocity depending on concentration $\phi$, at *s=1* and *s=3*, when an effective viscosity is calculated through the formula (2.1).

**Table 1**

| $\phi$ / *s* | | 0 | 0.1 | 0.2 | 0.3 |
|---|---|---|---|---|---|
| 1 | *c (cm/sec)* | 882 | 855 | 824 | 793 |
| 3 | *c (cm/sec)* | 895 | 889 | 905 | 901 |

Table 2 for the similar case shows the values for the damping coefficient depending on $\phi$.

**Table 2**

| $\phi$ / *s* | | 0 | 0.1 | 0.2 | 0.3 |
|---|---|---|---|---|---|
| 1 | $\delta_1$ *(1/sec)* | 0.0017 | 0.0025 | 0.0038 | 0.0039 |
| 3 | $\delta_1$ *(1/sec)* | 0.0018 | 0.0026 | 0.0035 | 0.0043 |

Table 3 for the same case shows the dependence of velocity amplitude of mixture flow for various volumetric concentrations.

**Table 3**

| $\phi$ / *s* | | 0 | 0.1 | 0.2 | 0.3 |
|---|---|---|---|---|---|
| 1 | $\lvert u_s \rvert$ *(cm/sec)* | 1.43 | 1.34 | 1.25 | 1.17 |
| 3 | $\lvert u_s \rvert$ *(cm/sec)* | 0.26 | 0.25 | 0.25 | 0.24 |

Based on received numerical calculations we can make the following conclusions:

- The wave velocity and the amplitude of flow velocity decrease with the increase of $\phi$.
- The biggest increase against concentration $\phi$ is observed for the coefficient $\delta_1$ (almost two times more)
- With the increase of harmonics the wave velocity increases.

## References

1. Dennis A. Siginer, Mario F. Letelier, Pulsating flow of visco-elastic fluids in straight tubes of arbitrary cross-section—Part II: secondary flows, International Journal of Non-linear Mechanics, vol. 37, iss. 2, pp. 395-407, 2002.
2. Fletcher C.A. Computational Techniques for Fluid Dynamics I, Springer-Verlag. 1988.
3. Вольмир А.С. Оболочки в потоке жидкости и газа. Задачи гидроупругости., М.: Наука, 1979. – 320 p.

4. Demiray H., Ercengiz. A. Wave propagation in a prestressed elastic tube filled with a viscous fluid. International Journal of Engineering Science, vol.29, iss.5, pp. 575-585, 1991.
5. Mitosek M. Oscillatory liquid flow in elastic porous tubes, J. Acta Mechanica, vol.101, N.1-4, pp.139-153, Springer, 1993.

Azerbaijan University of Architecture and Construction
ISSN 2706-7726
Engineering Mechanics
Scientific and Technical Journal
E-mail: engineeringmechanics@azmiu.edu.az

| September 2023 | Issue 14 | Volume 6 | Number 2 | Pages 20-25 |
|---|---|---|---|---|

# CONICAL COVER REINFORCED WITH NETTING RIBS, SPRING CONNECTED TO NON-ALLOY ELASTIC MEDIA A STUDY OF DANCE WITH THE MASS

**H. SH. MATANAGH**
*Azerbaijan University of Architecture and Construction, doctoral student,*
*hossein.shafiei.m@gmail.com*

**Abstract-***Conical structures are widely used in various engineering fields. As the engineering devices to which such constructions are applied are special-purpose devices, they can carry different: homogeneous elastic, homogeneous viscoelastic and non-homogeneous environments. On the other hand, in transport devices made of conical covers (containers, ballast tanks), a heavy mass load is used, which is attached to the body of the cover with a plateau inside, to prevent the vibrations and oscillations that occur during movement from reaching the resonance frequency. The presented article is devoted to the study of joint oscillations of a conical cover reinforced with mesh ribs in an inhomogeneous elastic medium with a mass connected to it by a spring.*
**Keywords:** *Conic shell, oscillations, viscoelastic medium, energetic method, Winkler model, Ferrari method.*

## I. Statement of the issue

Let's assume that a conical cover oscillating together with a mass connected by a spring in a homogeneous elastic medium and in a homogeneous non-homogeneous elastic medium is reinforced with ribs forming a network (Fig. 1.).

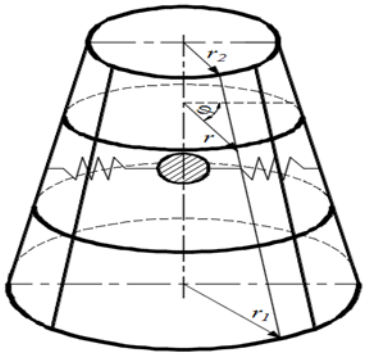


Figure 1. A mass-reinforced, inhomogeneous viscoelastic, conical cover in contact with the medium, reinforced with web-forming ribs.

## II. Problem solving

We look for the displacements of the points of the cover in the figure (1) [1]

$$w=\frac{(r_2+x\sin\gamma)^2}{r_1^2}\sin\frac{m\pi x}{l}\sum_{n=1}^{\infty}A_n(t)\cos n\varphi;$$

$$\vartheta=\frac{(r_2+x\sin\gamma)^2}{r_1^2}\sin\frac{m\pi x}{l}\sum_{n=1}^{\infty}B_n(t)\sin n\varphi \qquad (1)$$

$$u=\frac{(r_2+x\sin\gamma)^2}{r_1^2}\cos\frac{m\pi x}{l}\sum_{n=1}^{\infty}D_n(t)\cos n\varphi$$

Here n- the wave numbers in the circular direction, along the m-generator, $A_n(t)$, $B_n(t)$, $D_n(t)$are unknown constants.

In the case of the Winkler model, for the potential and kinetic energy of a conical cover in contact with a non-homogeneous elastic medium reinforced with ribs forming a network, together with the mass connected to it by a spring, we get [1, 2, 3]:

$$q_r=k(r)w=k_0(1-\xi\frac{x}{l})w=k_0(1-\xi\frac{x}{l})w=$$
$$=k_0(1-\xi\frac{r-r_2}{l\sin\gamma})w=k_0(1-\xi\frac{r-r_2}{r_1-r_2})w \qquad (2)$$

In the case of Winkler's model, let's write the sum of the potential and kinetic energies, that is, the expression of the total energy, for the nth aggregate of the rows included in the row (1):

$$L_{şv}=\mu_{11}D_n^2(t)+\hat{\mu}_{22}A_n^2(t)+\mu_{33}B_n^2(t)+\mu_{44}A_n(t)D_n(t)+\mu_{55}A_n(t)B_n(t)+$$
$$+\left(z-w_0\cos\gamma\right)^2c+\frac{1}{2}M\dot{z}^2+\mu_{66}A_n^{'2}+\mu_{77}D_n^{'2}+\mu_{88}B_n^{'2}. \qquad (3)$$

Here, and $\hat{\mu}_{22}$, $\mu_{33}$, $\mu_{44}$, $\mu_{55}$, $\mu_{66}$, $\mu_{77}$, $\mu_{88}$limits are given in the author's published articles [4, 5, 6] separately for the cases of reinforcement with longitudinal and transverse ribs. In the reviewed article, their sum is used. Since those statements are rather complex and voluminous, they are referred only to the author.

$$\frac{d}{dt}\left(\frac{\partial L_{şv}}{\partial\dot{q}_i}\right)-\frac{\partial L_{şv}}{\partial q_i}=0, \qquad (5)$$

(5) Substituting in the Lagrange equation, we get a system consisting of the following ordinary differential equation in the case of the Winkler model for inhomogeneous media reinforced by ribs forming a network:

$$M\ddot{z}+2c\left(z-\alpha_0A_n(t)\right)=0$$
$$-2\alpha_0cz+2\mu_{66}A_n^{''}(t)+(2\hat{\mu}_{22}+2\alpha_0^2c)A_n(t)+\mu_{44}D_n(t)+\mu_{55}B_n(t)=0$$
$$2\mu_{77}D_n^{''}(t)+2\mu_{11}D_n(t)+\mu_{44}A_n(t)=0 \qquad (6)$$
$$2\mu_{88}B_n^{''}(t)+2\mu_{33}B_n(t)+\mu_{55}A_n(t)=0$$

Burada, $\alpha_0=\frac{r_0^2}{r_1^2}\sin\frac{m\pi(r_0-r_2)}{r_1-r_2}\cos\gamma, n=1,3,5,\ldots$

In order to find specific oscillation frequencies in the case of the Winkler model of a conical cover reinforced with web-forming ribs, in contact with a non-homogeneous elastic medium, together with a mass connected to it by a spring, the solution of the system (6) is həllini $z=z^*\sin\omega t, A_n=A_n^*\sin\omega t, B_n=B_n^*\sin\omega t, D_n==D_n^*\sin\omega t$ sinωt and write instead in the system, we get a system of algebraic equations considering the constants $z^*, A_n^*, B_n^*, D_n^*$ taking into account the constants, we get a system of algebraic equations:

$$\left(\frac{2c}{M}-\omega^2\right)z^*-\frac{2c\alpha_0}{M}A_n^*=0$$

$$-2\alpha_0 cz^*+(2\hat{\mu}_{22}-2\mu_{66}\omega^2+2\alpha_0^2 c)A_n^*+\mu_{44}D_n^*+\mu_{55}B_n^*=0$$

$$(2\mu_{11}-2\mu_{77}\omega^2)D_n^*+\mu_{44}A_n^*=0 \qquad (7)$$

$$(2\mu_{33}-2\mu_{88}\omega^2)B_n^*+\mu_{55}A_n^*=0$$

Since the system (7) is a system of homogeneous linear algebraic equations, a necessary and sufficient condition for the existence of its non-trivial solution is that its principal determinant is equal to zero. As a result, in the case of the Winkler model of a conical cover in contact with an inhomogeneous elastic medium reinforced by meshing ribs with a mass attached to it by a spring, we obtain the following frequency equation to find the specific oscillation frequencies:

$$\left(\frac{2c}{M}-\omega^2\right)[\mu_{44}^2(2\mu_{33}-2\mu_{88}\omega^2)+\mu_{55}^2(2\mu_{11}-2\mu_{77}\omega^2)-(2\hat{\mu}_{22}-2\mu_{66}\omega^2+2\alpha_0^2 c)\times$$

$$\times(2\mu_{11}-2\mu_{77}\omega^2)(2\mu_{33}-2\mu_{88}\omega^2)]+2\alpha_0 c\varphi_{88}\omega^2-4\alpha_0 c\varphi_{33}=0 \qquad (8)$$

Note that when c = 0 or M = 0, equation (8) expresses the oscillation equation of the reinforced cross-section conical cover in contact with the environment, let's write it as follows:

$$\omega^6-(8\mu_{33}\mu_{66}\mu_{77}+4\hat{\mu}_{22}\mu_{77}\mu_{88}-4\mu_{11}\mu_{66}\mu_{88})(8\mu_{66}\mu_{77}\mu_{88})^{-1}\omega^4+$$

$$+(-2\mu_{88}\mu_{44}^2-2\mu_{77}\mu_{55}^2+4\hat{\mu}_{22}\mu_{33}\mu_{77}-4\mu_{11}\mu_{33}\mu_{66}+$$

$$+8\mu_{11}\hat{\mu}_{22}\mu_{33}+2\alpha_0 c\mu_{88})(8\mu_{66}\mu_{77}\mu_{88})^{-1}\omega^2+$$

$$+(2\mu_{33}\mu_{44}^2+2\mu_{11}\mu_{55}^2-8\mu_{11}\hat{\mu}_{22}\mu_{33}-4\alpha_0 c\mu_{33})(8\mu_{66}\mu_{77}\mu_{88})^{-1}=0. \qquad (9)$$

(9) tənliyini $\omega^2=\lambda$ –ya nəzərən kub tənlikdir:

$$\lambda^3+\tilde{f}_1\lambda^2+\tilde{f}_2\lambda+\tilde{f}_3=0 \qquad (10)$$

Here,

$$\tilde{f}_1=-(8\mu_{33}\mu_{66}\mu_{77}+4\hat{\mu}_{22}\mu_{77}\mu_{88}-4\mu_{11}\mu_{66}\mu_{88})(8\mu_{66}\mu_{77}\mu_{88})^{-1}$$

$$\tilde{f}_2=(-2\mu_{88}\mu_{44}^2-2\mu_{77}\mu_{55}^2+4\hat{\mu}_{22}\mu_{33}\mu_{77}-4\mu_{11}\mu_{33}\mu_{66}+8\mu_{11}\hat{\mu}_{22}\mu_{33}+$$

$$+2\alpha_0 c\mu_{88})(8\mu_{66}\mu_{77}\mu_{88})^{-1};.$$

$$\tilde{f}_3=(2\mu_{33}\mu_{44}^2+2\mu_{11}\mu_{55}^2-8\mu_{11}\hat{\mu}_{22}\mu_{33}-4\alpha_0 c\mu_{33})(8\mu_{66}\mu_{77}\mu_{88})^{-1}$$

Using the Cardano formula, we can find the roots of the cubic equation (10):

$$\lambda=y-\frac{\tilde{f}_1}{3}$$

$$y=\sqrt[3]{-\frac{\tilde{q}}{2}+\sqrt{\frac{\tilde{q}^2}{4}+\frac{p^3}{27}}}+\sqrt[3]{-\frac{\tilde{q}}{2}-\sqrt{\frac{\tilde{q}^2}{4}+\frac{p^3}{27}}}$$

$$p=\frac{-\tilde{f}_1^2}{3}+\tilde{f}_2;\tilde{q}=\frac{2\tilde{f}_1^3}{27}-\frac{\tilde{f}_1\tilde{f}_2}{3}+\tilde{f}_3.$$

Equation (10) is an eight-order equation with respect to ω^2=λ:

$$8\mu_{66}\mu_{77}\mu_{88}\omega^8-\left(\bar{T}_1+\frac{16c}{M}\mu_{66}\mu_{77}\mu_{88}\right)\omega^6+\left(\bar{T}_2+\frac{2c}{M}\bar{T}_1-\right.$$

$$\left.-16c^2\propto_0^2\mu_{77}\mu_{88}\right)\omega^4-\left(\bar{T}_3+\frac{2c}{M}\bar{T}_2+16c^2\propto_0^2\mu_{11}\mu_{88}+16c^2\propto_0^2\mu_{33}\mu_{77}\right)\omega^2-$$

$$-\frac{2c}{M}\bar{T}_3-16c^2\propto_0^2\mu_{33}\mu_{77}=0$$

$$\bar{T}_1=8\hat{\mu}_{22}\mu_{77}\mu_{88}+8\mu_{11}\mu_{66}\mu_{88}+8\mu_{66}\mu_{77}+8c^2\propto_0^2\mu_{88}\mu_{77}+$$

$$\bar{T}_2=-2\mu_{44}^2\mu_{88}-2\mu_{55}\mu_{77}+8\hat{\mu}_{22}\mu_{11}\mu_{88}+8\hat{\mu}_{22}\mu_{33}\mu_{77}+8\mu_{11}\mu_{33}\mu_{66}+$$

$$+8c^2\propto_0^2\mu_{11}\mu_{88}+8c^2\propto_0^2\mu_{33}\mu_{77}$$

$$\bar{T}_3=2\mu_{33}\mu_{44}^2+2\mu_{11}\mu_{55}-8\hat{\mu}_{22}\mu_{11}\mu_{33}-8c^2\propto_0^2\mu_{11}\mu_{33}$$

This equation is a quadratic algebraic equation with respect to $\lambda=\omega^2$:

$$8\mu_{66}\mu_{77}\mu_{88}\lambda^4-\left(\bar{T}_1+\frac{16c}{M}\mu_{66}\mu_{77}\mu_{88}\right)\lambda^3+\left(\bar{T}_2+\frac{2c}{M}\bar{T}_1-\right.$$

$$\left.-16c^2\propto_0^2\mu_{77}\mu_{88}\right)\lambda^2-\left(\bar{T}_3+\frac{2c}{M}\bar{T}_2+16c^2\propto_0^2\mu_{11}\mu_{88}+16c^2\propto_0^2\mu_{33}\mu_{77}\right)\lambda-$$

$$-\frac{2c}{M}\bar{T}_3-16c^2\propto_0^2\mu_{33}\mu_{77}=0$$

The last equation can be solved by the Ferrari method. Let's show it like this:

$$\lambda^4+\bar{A}\lambda^3+\bar{B}\lambda^2+\bar{C}\lambda+\bar{D}=0 \qquad (11)$$

Here,

$$\bar{A}=(8\mu_{66}\mu_{77}\mu_{88})^{-1}\left(\bar{T}_1+\frac{16c}{M}8\mu_{66}\mu_{77}\mu_{88}\right);\ \bar{D}=-\frac{2c}{M}\bar{T}_3-16c^2\propto_0^2\mu_{33}\mu_{77}$$

$$\bar{B}=(8\mu_{66}\mu_{77}\mu_{88})^{-1}\left(\bar{T}_2+\frac{2c}{M}\bar{T}_1-16c^2\propto_0^2\mu_{77}\mu_{88}\right)$$

$$\bar{C}=(8\mu_{66}\mu_{77}\mu_{88})^{-1}\left(\bar{T}_3+\frac{2c}{M}\bar{T}_2+16c^2\propto_0^2\mu_{11}\mu_{88}+16c^2\propto_0^2\mu_{33}\mu_{77}\right)$$

First of all

$$y^3-\bar{B}y^2+(\bar{A}\bar{C}-4\bar{D})y-\bar{A}^2\bar{D}+4\bar{B}\bar{D}-\bar{C}^2=0$$

any solution of the equation is found.

The roots of the received equation (11) were calculated using a numerical method. The following values are taken for the parameters: $r_1=160$ мм, $r_2=85$мм, the rings are taken as angular 6×10×1 (in mm), $k_1=32, k_2=15\ m=1,\ \gamma=\frac{13\pi}{180}$ , the height of the cover 320 mm is accepted.

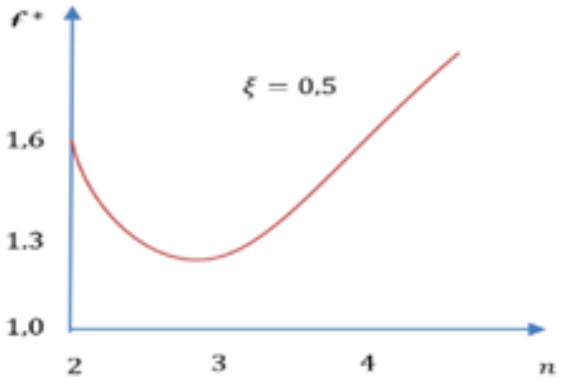


Figure 2. Dependence of the specific oscillation frequencies of the cover on the wave number in the circular direction

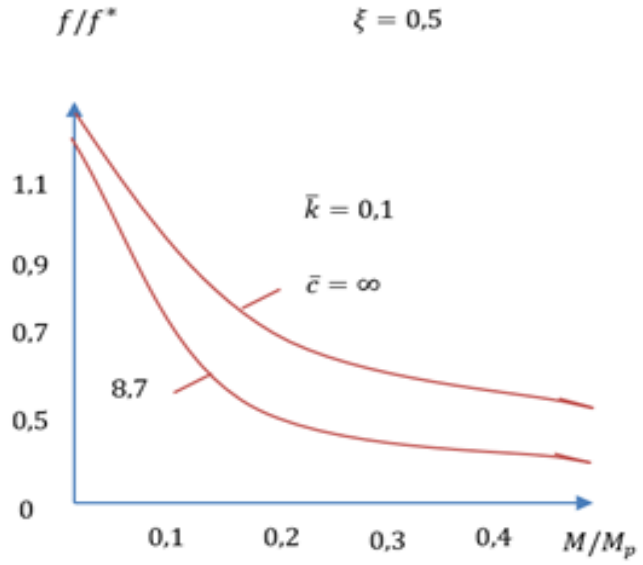


Figure 3. Dependence of specific oscillation frequencies of the coating on the mass of the loa

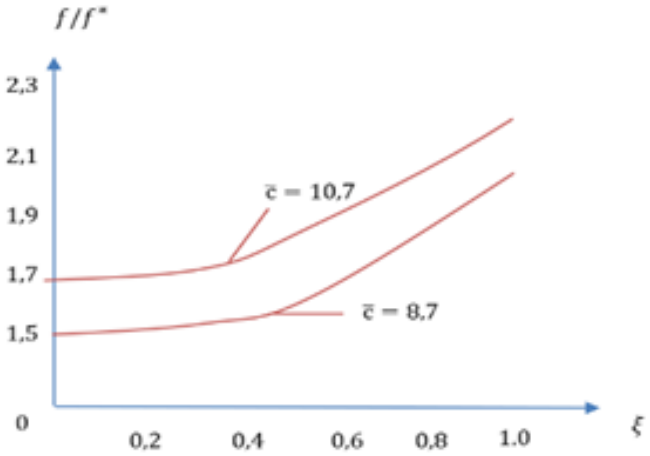


Figure 4. Dependence of specific oscillation frequencies of the coating on the inhomogeneity parameter of the environment.

**III. Results**

The results of the calculations are shown in figure 2 as the frequency parameter $f^* = \frac{\omega}{2\pi}$ from n, in figure 3 the ratio of the ratio of the minimum specific oscillation frequencies of the system to the minimum specific oscillation frequencies of the cover reinforced with ribs in the form of dependence on the mass of the load is different $\bar{k}$=k /D values and $\bar{c}$=c/D are given. Figure 3 shows the dependence of the minimum specific oscillation frequencies of the system on the environment inhomogeneity parameter. As can be seen from Figure 2, as the number of n increases, the minimum specific oscillation frequencies of the system first decrease, and then increase to a minimum value. Figure 3 shows that the *M/Mp* ratio (*Mp*-cover is its mass with ribs) increases, the minimum specific oscillation frequencies of the system decrease, and vice versa, as the ratio $\bar{k}$=k_0/D increases and the stiffness of the spring increases, the minimum specific oscillation frequencies of the system increase. This is explained by the fact that an increase in the ratio $\bar{k}$=k_0/D leads to an increase in the hardness of the medium. As can be seen from Figure 4., as the value of the environment inhomogeneity parameter increases, the specific oscillation frequencies of the system decrease. The reason for this is the increase in the value of the non-homogeneity parameter of the environment, which leads to an increase in the hardness of the environment.

**Literature**

1. Shafiei, H. M. Free oscillations of a conical roof reinforced with longitudinal bars with a spring-connected load with the environment // Modern problems of construction and construction education, 2017.19-21 December.
2. Iskanderov R.A., Shafiei Matanagh H.M. Free vibrations of longitudinally reinforced conical shell with spring associated mass in medium// Problems of computational mechanics and strength of structures, Dnepropetrovsk National University named after Oles Honchar, vol.26,2017.
3. Iskanderov R.A., Shafiei Matanagh H.M. Free vibrations of lateral reinforced conical shell with spring associated mass in medium/ Conference proceedings. The 13th International Conference on Technical and Physical Problems of Electrical Engineering September 21-23, 2017 Van, Turkey.
4. Iskanderov R.A., Shafiei Matanagh H.M. Free vibrations of lateral reinforced conical shell with spring associated mass in medium /IJTPE Journal International Journal on Technical and physical problems of engineering, Issue 32 Volume 9 Number 3 p. 48-52, September 2017, Denmark.
5. Iskanderov RA, H. Shafiei Matanagh. Free vibrations of a conical shell with spring associated mass and stiffened with a cross system of ribs in medium. International Journal on "Technical and Physical Problems of Engineering" (IJTPE), Issue 43, Vol.12, Number 2, Pages 1-5, June 2020
6. Shafiei Matanagh H. M. Free vibrations of a longitudinally supported conical shell with a mass attached to springs in contact with an inhomogeneous medium// Problems of Computational Mechanics and Strength of Structures, Vol. 29, pp. 221-234, 2019.

Azerbaijan University of Architecture and Construction
ISSN 2706-7726
Engineering Mechanics
Scientific and Technical Journal
E-mail: engineeringmechanics@azmiu.edu.az

| September 2023 | Issue 14 | Volume 6 | Number 2 | Pages 25-28 |
|---|---|---|---|---|

# OPTIMIZATION OF THE PARAMETERS OF A NON-MOLICY, FREELY DANCED CYLINDRICAL SHELL WITH A FLUID IN THE DIRECTION OF THE COORDINATE AXES

**Javad Mahdavi Tabatabaei**
*Department of Mechanics, Azerbaijan University of Architecture and Construction,*
*nadermt@gmail.com*

**Abstract-** *In practice, depending on working conditions, cylindrical coatings of different hardness are obtained by adding different mixtures in technological processes. Due to such additives, depending on the composition of the material, a sharp inhomogeneity and anisotropy feature occurs in the materials of the constructions. Therefore, one of the most important issues in the report of the mentioned constructions is to evaluate the mechanical properties of the construction element as correctly as possible. On the other hand, such constructions are in contact with environments of different nature. The conducted studies show that taking into account the influence of the environment is important in solving dynamic issues.*

**Key words:***Inhomogeneity, Bubnov Galerkin's method, Kirchhoff-Liav hypothesis, frequency parameter, optimization.*

## I. INTRODUCTION

Let's give a brief summary of the work related to the topic discussed in the presented article. In the work of [1], an approximate-analytical solution method was established for solving free oscillations taking into account the resistance of plates with different configurations and plates made of continuous inhomogeneous orthotropic materials with a circular cross-section, and the resistance of the cylindrical coating to the external environment with complex properties. In the work of [2], the oscillating movements of non-homogeneous rectangular plates are studied taking into account the resistance of the external environment. In [3], the equations of motion of continuous non-homogeneous rectangular plates with constant thickness, whose modulus of elasticity and density depend on three-space coordinates, were derived for the orthotropic case. It is considered here that the Kirchhoff-Liav hypothesis can be accepted for an inhomogeneous orthotropic plate. In [7], the modulus of elasticity and density depend on the coordinates directed along the plane of the plate and are located on a viscoelastic base. Since the equation of motion is a special derivative linear equation with variable coefficients, separation into variables and Bubnov-Galerkin methods were used. A report was made on the specific values of the characteristic parameters, the results, tables, and the relationship curves between the parameters characterizing the properties of the material and the base were constructed. In [6], the problem of free oscillations of a rectangular plate with variable thickness was solved taking into account the resistance of the external environment, and a report was made on the variation of the characteristic functions with a linear law in the first approximation. The results of the report are presented in tables and links. In the work of [6], it is considered that the elasticity coefficients of the plate, the density change with a linear law along the length and thickness of the plate. The solution of the problem was solved with the help of separation into variables and orthogonalization methods of Bubnov Galerkin. In the works of [6, 7], it is dedicated to the solution of the problems of oscillation motions of a non-homogeneous orthotropic circular plate

and a cylindrical cover with a circular cross-section, taking into account the resistance of the external environment. The solution of the problem is brought to the solution of the system of linear equations. In the received system equation, it is possible to eliminate the stress function and, due to the distortion, the six-form variable coefficient is brought to the special derivative equation. By dividing the solution of the problem into its variables and using the Bubnov Galerkin method, the value of the frequency is determined, and the effect of the non-homogeneity of the material and the base is investigated in special cases.

## II. STATEMENT OF THE ISSUE

The system in [3,4,5] works of the considered problem was solved by the author of equation (1), which allows finding the oscillation frequency

$$4\gamma_{11}\gamma_{22}\gamma_{33}+\gamma_{44}\gamma_{55}\gamma_{66}-\gamma_{55}^2\gamma_{22}-\gamma_{66}^2\gamma_{11}-\gamma_{44}^2\gamma_{33}=0. \quad (1)$$

found roots allow choosing the optimal variant of the studied construction.

Equation (1) was obtained with the help of the following approach.

$$J_{ch*}=\gamma_{11}u_0^2+\gamma_{22}\vartheta_0^2+\gamma_{33}w_0^2+\gamma_{44}u_0\vartheta_0+\gamma_{55}u_0w_0+\gamma_{66}\vartheta_0w_0 \quad (2)$$

Denoting the total energy of the system[3,4,5 ]Functionality is not original $u_0,\vartheta_0,w_0$ if we vary with respect to the constants and make the coefficients of independent variations equal to zero, we get the following system of homogeneous equations:

$$\begin{cases}2\gamma_{11}u_0+\gamma_{44}\vartheta_0+\gamma_{55}w_0=0\\ \gamma_{44}u_0+2\gamma_{22}\vartheta_0+\gamma_{66}w_0=0\\ \gamma_{55}u_0+\gamma_{66}\vartheta_0+2\gamma_{33}w_0=0\end{cases} \quad (3)$$

Since the system (3) is a system of homogeneous equations, a necessary and sufficient condition for the existence of its non-zero solution is that the main determinant is equal to zero. As a result, we get the following frequency equation:

$$\begin{vmatrix}2\gamma_{11} & \gamma_{44} & \gamma_{55}\\ \gamma_{44} & 2\gamma_{22} & \gamma_{66}\\ \gamma_{55} & \gamma_{66} & 2\gamma_{33}\end{vmatrix}=0 \quad (4)$$

Let's write equation (4) as follows:

$$4\gamma_{11}\gamma_{22}\gamma_{33}+\gamma_{44}\gamma_{55}\gamma_{66}-\gamma_{55}^2\gamma_{22}-\gamma_{66}^2\gamma_{11}-\gamma_{44}^2\gamma_{33}=0. \quad (5)$$

Since the unknown frequency parameter is included in the argument of the Bessel function, equation (5) is a transcendental equation. It was calculated by numerical method. Finding the roots of the equation is based on the sign change of the numbers obtained from the calculation at different values of the frequency parameter of the left side of the equation (5). By changing the sign of the left side of the equation, the interval where the root is located is determined, and then the root is calculated using Newton's method.

The found roots of equation (5) allow choosing the optimal variant of the studied structure. That is, the goal is how to adjust the number of spindles and rings, the thickness of the cylindrical cover, so that the chosen structure is lighter in weight, has a lower cost from an economic point of view, and has a strength that meets the needs of practice. A relative efficiency factor or optimization parameter for this $\mu$ is included. As such a parameter, the ratio of the square of the minimum specific oscillation frequency of a cylindrical cover reinforced with discretely distributed shafts and rings, in contact with a liquid, the material of which has different inhomogeneity properties in the direction of the coordinate axes, to the square of the specific oscillation frequency of a smooth cylindrical cover of the same weight as them is taken:

$$\mu = \frac{\omega_{1\min}^2}{\omega_{10\min}^2} \qquad (6)$$

The solution to the problem is the relative thickness of the coating $h^* = \frac{h}{R}$, the ratio of the distances between shafts to the thickness of the shaft $a_1 = \frac{2\pi R}{k_1 h_i}$, the ratio of the distances between the rings to the thickness of the ring $a_2 = \frac{L_1}{(k_2+1)h_j}$, the ratio of the weight of the spindles to the weight of the rings $\varphi_2'$, the ratio of the total weight of the ribs to the weight of the cover $\varphi_1'$ at different values of its parameters $\mu$ is brought to find the maximum value of the parameter. The dimensions and material of the cover with the maximum value of this ratio are considered optimal.

Found from equation (5) in Graph 1 $\omega_1$ optimization parameters based on frequencies $\mu$ – The calculated values of different $\varphi_2'$ for s $\varphi_1'$ Originated from In the graph, solid lines correspond to the cases where the non-homogeneity of the material of the cylindrical cover reinforced with ribs is taken into account by a linear law, and the broken lines correspond to the cases where the material of the cylindrical cover reinforced with ribs is homogeneous. The dotted lines represent the exponential of the material inhomogeneity of the rib-reinforced cylindrical cover.indicates a suitable case where it is considered to be changed by law.Calculations show that the optimal version of the construction $\mu_{\max} = 22,14$ the price is right. As can be seen from graph 1 $\varphi_1'$ as it increases heThe value of the optimization parameter increases, reaches a maximum value, and then decreases again. Corresponding to the maximum of the optimization parameter $\varphi_1'$ of the price varies around the unit. This indicates that the weight of the ribs is approximately equal to the weight of the cylindrical cover

strengthening the shell is more effective when As can be seen from the graph $\varphi_1'$ -at small prices of $\mu$ parameter unitan thatChminimum priceabuy tir which is cylindricalshows that reinforcing the shell with extremely weak shafts is not efficient. Optimization parameter $\mu$ of

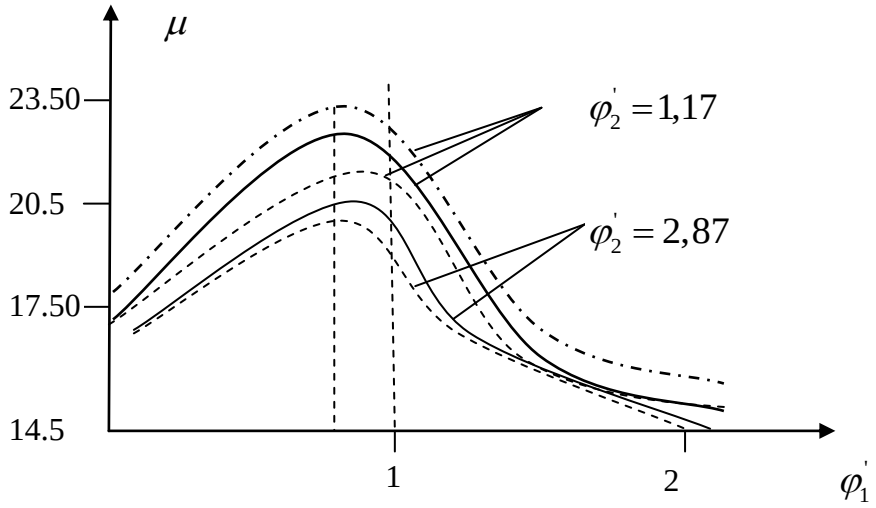


Fiqure 1. Relative efficiency

ratio $\mu$ the ratio of the rods of weight $\varphi_1^{'}$ dependence on $\varphi_2^{'}$ shows that the dependence on $\mu$ the maximum value of the parameter $\varphi_2^{'} > 1$ and in the example we are looking at $\varphi_2^{'} = 1{,}17$ is equal toCalculations show that the non-homogeneity property of the material of the cylindrical coating changes with an exponential law and is more favorable than the case with a linear law. In the event that the inhomogeneity property of the material of the cylindrical coating varies with the exponential law $\mu_{\max} = 23{,}11$ is equal to

## RESULTS

In the article, the problems of free oscillations of the reinforced cylindrical shell with different inhomogeneity properties in the direction of the coordinate axes and of the reinforced cylindrical shell with the "sharp" inhomogeneity property in the direction of the coordinate axes are solved together with the soil. Cases of inhomogeneity functions changing with linear and exponential laws were considered.

As the inhomogeneity property in the direction of the cylindrical shell increases, the free oscillation frequencies of the reinforced cylindrical shell-fluid system increase.

As the number of shafts increases, the difference between the free oscillation frequencies of the shaft-reinforced cylindrical shell with fluid, which varies exponentially in the direction of the inhomogeneity law axes, and the corresponding free oscillation frequencies of the cylindrical shell reinforced with shafts, which varies linearly in the direction of the inhomogeneity law axes, decreases.

The case of the inhomogeneity property of the material of the cylindrical coating changing with an exponential law is more favorable than the case changing with a linear law. Optimization parameter in the case of exponentially changing material inhomogeneity of the cylindrical coating $\mu_{\max} = 23{,}11$ to , and in the case of changing with a linear law $\mu_{\max} = 22{,}0$ is equal to

At a positive value of the inhomogeneity parameters, the specific oscillation frequencies of the system increase compared to the specific oscillation frequencies corresponding to the homogeneity, and at a negative value, they decrease.

Consideration of soil viscosityof free oscillation frequencies of the systemthe force acting on the cylindrical cover by the environment decreases compared to the elastic case.

## REFERENCES

1. Hajiyev VC, Mirzoeva GR, Shiriyev AJ// Effect of Winkler foundation, inhomogeneity and orthotropic on the frequency of plates// Journal pledge of structural Engineering Mechanics, 2018, volume 1, Iggue pages 1-5.

2. Hajiyev VC, Sofiyev AH, Kuruoglu//Free bending vibration analysis of thin bidirectional exponentially graded orthotropic rectangular plates resting on two parameter elastic foundations//Composite Structures 2018, pp. 372-377.

3. Haciyev VC, Sofiyev AH, Kuruoglu-On the vibration of orthotropic and inhomogeneous with spatial coordinates plates resting on the inhomogeneous viscoelastic foundation// Mechanics of Advanced Materials and structures, 2018, vol 0.N00, pp. 1-12.

4. Iskanderov RA, Tabatabaei JM. Vibrations of fluid-filled inhomogeneous cylindrical shells strengthened with lateral ribs. IJTPE Journal International Journal on Technical and physical problems of engineering October 14-15, 2019, Istanbul, Turkey, p. 206-210.

5. Iskanderov RA, Tabatabaei JM. Vibrations of fluid-filled inhomogeneous cylindrical shells strengthened with lateral ribs.International Journal on "Technical and Physical Problems of Engineering" (IJTPE)March 2020, Issue 42, Volume 12, Number 1, Pages 121-125.

6. Iskanderov RA, Tabatabaei JM Vibrations of fluid-filled inhomogeneous cylindrical shells strengthened with lateral ribs.International Journal on "Technical and Physical Problems of Engineering" (IJTPE) June 2020, Issue 43, Volume 12, Number 2, Pages 121-125.

7. Shiriev A.I. On the vibration of a rectangular plate of variable thickness lying on a viscoelastic base//Vestnik of Baku University. Physico-Math. Nauki, No. 3, 2015, pp. 128-133

Azerbaijan University of Architecture and Construction
ISSN 2706-7726
Engineering Mechanics
Scientific and Technical Journal
E-mail: engineeringmechanics@azmiu.edu.az

| September 2023 | Issue 14 | Volume 6 | Number 2 | Pages 29-33 |
|---|---|---|---|---|

# THE ORIGIN OF A CRACK IN THE STRIP DURING UNEVEN HEATING

**R. A. Allahverdiev, B.M. Aslanov**
*Azerbaijan University of Architecture and Construction,*
a.r_1984@mail.rut, atiahi-amiu-thik@mail.ru

**Abstract-** *Strips (rods) are widely used in products and structures for various purposes. Very often they are subject to thermal stress. For practice, it is important to study the origin of cracks in a strip (rod) during uneven heating. Based on the methods of elasticity theory, a mathematical description of the calculation model for the occurrence of a crack in a strip (beam) is carried out when the strip is bent in its plane by a given system of external loads (constant bending moments, uniformly distributed pressure, etc.). The process of destruction of real materials is complex and occurs differently for different materials. This depends on the structure of the material, its chemical composition, type of voltage, and others.*

**Keywords**: *Origin of cracks, uneven heating, isotropic strip, thermal load, stress-strain state*

**Formulation of the problem.**

Let us consider a homogeneous isotropic strip (rod). Let us denote by 2c and 2h the width and thickness of the strip, respectively. The choice of Cartesian coordinate system and notation are explained in Fig. 1. The Cartesian coordinates xy in the midplane of the strip are the plane of symmetry. Let the strip (rod) be subjected to uneven heating across the width of the cross section. We will assume that the temperature of the strip is only a function of the x coordinate and does not depend on other coordinates.

As the strip (rod) is loaded with a thermal load, pre-fracture zones will appear, which we model as areas of weakened interparticle bonds of the material. We will study the initiation of a crack in a strip (rod) under the influence of uneven heating on the basis of a model of a pre-fracture zone with connections between the edges [8,11]. Let us consider the case when the pre-fracture zone is directed perpendicular to the side edges of the strip (Fig. 1). It is believed that the edges of the strip parallel to the hou plane are free from external stresses. The interaction of the banks of the pre-fracture zone is modeled by introducing bonds between the banks of the pre-fracture zone that have a given deformation diagram. The physical nature of such bonds and the size of the pre-fracture region depend on the type of material. In the general case, it represents a nonlinear law of deformation [3, 10].

In the case under study, the occurrence of a crack is the process of transition of the pre-fracture region into the region of broken bonds of the material between the surfaces of the strip medium. In this case, the size of the pre-fracture area is unknown in advance and must be determined in the process of solving the problem. The pre-fracture zone is oriented in the direction of the maximum tensile stresses that arise in the rod under the action of uneven heating.

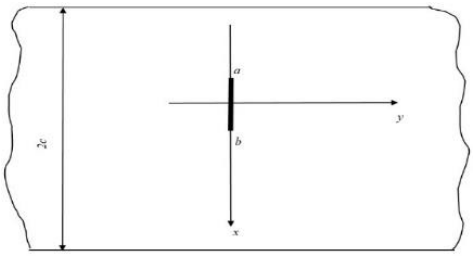

Let the x-axis of the 0xy coordinate system be aligned with the line of the pre-fracture zone ( $a \le x \le b$ ). The shores of the pre-fracture zone interact in such a way that this interaction (connections between the shores) inhibits the initiation of a crack. For a mathematical description of the interaction between the shores of the pre-fracture zone, we assume that between the shores there are connections (adhesive forces between particles of the rod material), the law of deformation of which is specified [1, 2].

The problem under consideration is to determine the stress-strain state of the rod, as well as to determine the maximum intensity of unequal heating (thermal load), upon reaching which a crack will appear.

Under the action of temperature stresses in the strip, forces will arise in the bonds connecting the banks of the pre-fracture zone. The magnitude of these stresses and the size of the pre-fracture zone are unknown in advance and must be determined in the process of solving the problem.

The boundary condition of the problem in the pre-fracture zone will be

$$\sigma_y = q(x);\ \ \tau_{xy} = 0, \text{ at } y = 0,\ a \le x \le b$$

We define the stress-strain state in the vicinity of the pre-fracture zone approximately in the sense [6] that we will satisfy the boundary conditions of the problem on the contour of the pre-fracture zone (conditions (1)), and require that at a considerable distance from the pre-fracture zone the stress state in the rod coincides with thermally stressed state caused by uneven heating for a continuous strip. The main relations of the problem posed must be supplemented with an equation connecting the opening of the banks of the pre-fracture strip and the forces in the connections. This equation, without loss of generality, in the problem under consideration can be represented in the form [8, 11]

$$\upsilon^+(x,0) - \upsilon^-(x,0) = C(x,q)q(x)$$

where $(\upsilon^+ - \upsilon^-)$ is the opening of the banks of the pre-fracture zone, x is the affix of the points of the banks of the pre-fracture zone; the function $C(x,q)$ can be considered as the effective compliance of the bonds, depending on the tension of the bonds.

**The solution of the problem.**

Let us imagine the desired stress state in the following form

$$\sigma_y = \sigma_y^0 + \sigma_y^1; \qquad \sigma_x = \sigma_x^0 + \sigma_x^1; \qquad \tau_{xy} = \tau_{xy}^0 + \tau_{xy}^1 \tag{3}$$

Here ( $\sigma_y^0$, $\tau_{xy}^0$ ) are the components of the stress tensor in the rod in the absence of a pre-fracture zone and caused by uneven heating; $\sigma_x^1$, $\sigma_y^1$, $\tau_{xy}^1$ - respectively, normal and tangential stresses caused by the presence of a pre-fracture zone in the rod.

For temperature stresses $\sigma_x^0$, $\sigma_y^0$, $\tau_{xy}^0$ we have

$$\sigma_x^0 = 0;\ \tau_{xy}^0 = 0;\quad \sigma_y^0 = -\alpha E T(x) + \frac{1}{2c}\int_{-c}^{c} \alpha E T(x)dx + \frac{3x}{2c^3}\int_{-c}^{c} \alpha E T(x)xdx \tag{4}$$

Here $\alpha$ is the coefficient of linear thermal expansion of the rod material; E is the elastic modulus of the material, T(x) is the temperature function.

To determine the introduced stresses $\sigma_x^1$, $\sigma_y^1$, $\tau_{xy}^1$ satisfying the equations of the plane theory of elasticity, we come to the boundary value problem

$$\sigma_y^1 + i\tau_{xy}^1 = f(x) + q(x) \quad \text{at } y = 0,\ a \le x \le b \tag{5}$$

Here

$$f(x) = \alpha ET(x) - \frac{1}{2c}\int_{-c}^{c} \alpha ET(x)dx - \frac{3x}{2c^3}\int_{-c}^{c} \alpha ET(x)xdx \tag{6}$$

As is known [9], the components of the stress tensor in the conditions of a plane problem in the theory of elasticity are expressed through two analytical functions $\Phi(z)$ and $\Psi(z)$. Based on the boundary conditions and Kolosov-Muskhelishvili relations [5, 6] to determine complex potentials, $\Phi(z)$ and $\Psi(z)$ we obtain the following boundary value problem:

$$\Phi(x) + \overline{\Phi(x)} + x\Phi'(x) + \Psi(x) = f_0(x), \quad \text{at } y = 0,\ a \le x \le b, \tag{7}$$

Where, $f_0(x) = f(x) + q(x)$

Let us introduce a new complex function

$$\Omega(z) = z\Phi'(z) + \Psi(z) \tag{8}$$

To determine the analytical functions and based on the boundary conditions $\Phi(z)$ and $\Psi(z)$ we obtain the following boundary value problem

$$\Phi(x) + \overline{\Phi(x)} + \Omega(x) = f_0(x), \quad \text{at } y = 0,\ a \le x \le b. \tag{9}$$

Since the stresses in the strip (rod) are limited, the solution to the boundary value problem (9) should be sought in the class of everywhere bounded functions. Due to the conditions of symmetry with respect to the x axis $f_0(x)$ the function is real, therefore, based on (9), on the entire real axis there will be

$$\operatorname{Im}\Omega(z) = 0$$

Consequently, taking into account the conditions at a considerable distance from the pre-fracture zone, we find

$$\Omega(z) = 0. \tag{10}$$

So, based on (10) for the function $\Phi(z)$ we obtain the Dirichlet problem

at

$$y = 0, \quad a \le x \le b \quad \operatorname{Re}\Phi(z) = \frac{1}{2} f_0(x),\ z \to \infty,\ \Phi(z) \to 0. \tag{11}$$

Boundary value problem (11) corresponds to the following problem of linear conjugation of boundary conditions [10]

$$\Phi^+(x) + \Phi^-(x) = f_0(x) \quad \text{on } a \le x \le b \tag{12}$$

It is required to find a solution (12) that satisfies the condition

$$\overline{\Phi}(z) = \Phi(z)$$

The corresponding homogeneous problem has the form

$$\Phi^+(x) + \Phi^-(x) = 0 \quad \text{on } a \le x \le b \tag{13}$$

For a particular solution of the homogeneous problem (13), we take the function

$$X(z) = \sqrt{(z-a)(z-b)}$$

meaning the branch for which equality holds

$$X^+(x) = -X^-(x) \quad \text{on } a \le x \le b \tag{14}$$

Based on relation (14), we rewrite the problem of linear conjugation of boundary values (13) as follows:

$$\frac{\Phi^+(x)}{X^+(x)} - \frac{\Phi^-(x)}{X^-(x)} = 0 \quad \text{on } a \le x \le b \tag{15}$$

From the boundary condition (15) it follows that the solution to a homogeneous problem that disappears at infinity is equal to zero.

We represent the inhomogeneous linear conjugation problem (12) in the following form

$$\frac{\Phi^{+}(x)}{X^{+}(x)}-\frac{\Phi^{-}(x)}{X^{-}(x)}=\frac{f_0(x)}{X^{+}(x)} \quad \text{on} \quad a\le x\le b \qquad (16)$$

Let's denote

$$\Phi_*(z)=\frac{\Phi(z)}{X(z)}; \qquad F_*(x)=\frac{f_0(x)}{X^{+}(x)},$$

then the boundary condition (16) will take the form

$$\Phi_*^{+}(x)-\Phi_*^{-}(x)=F_*(x) \quad \text{on} \quad a\le x\le b$$

The desired solution to the problem will be written as follows

$$\Phi(z)=\frac{\sqrt{(z-a)(z-b)}}{2\pi i}\int_a^b\frac{f_0(x)}{\sqrt{(x-a)(x-b)}(x-z)}dx \qquad (17)$$

The size of the pre-fracture zone (parameters a and b) can be determined from the solvability conditions of the boundary value problem

$$\int_a^b\frac{f_0(x)dx}{\sqrt{(x-a)(x-b)}}=0;\int_a^b\frac{xf_0(x)dx}{\sqrt{(x-a)(x-b)}}=0 \qquad (18)$$

System of equations (18) allows us to determine the unknown parameters a and b (the size of the pre-fracture zone).

We obtain the conditions for the solvability of problem (18) in the following form

$$\sum_{k=1}^{M}f_0(\tau_k)=0;\sum_{k=1}^{M}\tau_k f_0(\tau_k)=0 \qquad (19)$$

We will assume that the rupture of bonds in the pre-fracture zone at the point x = x0 occurs when the condition is met

$$\upsilon^{+}(x_0,0)-\upsilon^{-}(x_0,0)=\delta_c. \qquad (20)$$

Where, are the characteristics of the material for resistance to cracking.

To $\delta_c$ determine the critical thermal state causing the appearance of a crack in the strip (rod) based on condition (20), we obtain the following equation

$$\frac{4}{\pi E}\int_a^b\frac{f_0(t)F_1(t,x)dt}{X(t)}=\delta_c \qquad \text{on} \quad a\le x\le b. \qquad (21)$$

It is obvious that the rupture between partial bonds of the material will occur in the middle part of the pre-fracture zone.

Let us transform equation (21) to a form convenient for numerical solution. Passing to dimensionless variables in the integrals and replacing the integrals with Gaussian quadrature formulas for Chebyshev nodes, we reduce equation (21) to the following form

$$\frac{4}{EM}\sum_{m=1}^{M}f_0(t_m)F_1(t_m,x)=\delta_c, \qquad (22)$$

In Fig. 2. graphs of the dependence of the dimensionless length of the pre-fracture zone on the temperature parameter ( - characteristic temperature of the strip) are presented. In the calculations it was assumed that v = 0.3; M = 30.

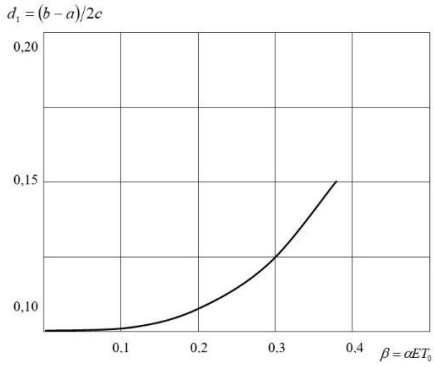


An effective method has been created for solving a class of problems in fracture mechanics about the occurrence and development of cracks in a strip under the influence of force and thermal loads. Based on the developed computational model;

a) the formation of cracks in strips under the influence of force and thermal loads was studied; b) a method is proposed for calculating the forces arising between the edges of zones of weakened interparticle bonds of the material in the strip; c) a method has been developed for calculating the opening of the banks of pre-collapse zones and cohesive cracks in a strip under the influence of force and thermal loads.

## REFERENCES

[1] I.A. Birger, "General algorithms for solving problems of the theory of elasticity, plasticity and creep", Successes of mechanics of deformable media, Nauka, pp. 51-75, Moscow 1975

[2] F.D. Gakhov, "Boundary value problems" , Nauka, 640 p., Moscow 1977

[3] R.V.Goldstein, M.N. Perelmuter, "Modeling of crack resistance of composite materials", Computational continuum mechanics, vol. 2, pp. 22-39, 2009

[4]"Achievements in the study of Destruction", Proceedings of the 9th International Conference on Destruction in Six volumes (English), vol. 1-6, 3122 p. Sydney, 1997

[5] A.A. Ilyushin, "Plasticity", LOGOS, 376 p., Mockow, 2004.

[6] V.A.Levin, E.M.Morozov, Yu.G.Matvienko, "Selected nonlinear problems of fracture mechanics" Fizmatlit, Mockow, 408 p. 2004

[7] Yu.G. Matvienko, "Physics and mechanics of destruction of solids", Editorial URSS, Moscow, 74 p., 2000

[8] M.V. Mir-Salim-zadeh, "The origin of a cracin a reinforced plate", Applied мechanics and theoretical physics, vol. 48, No. 4, pp. 111 – 120, 2007

[9] V.M. Mirsalimov, "Inhomogeneous elastoplastic problems", Nauka, Mockow, 256 p, 1987

[10] V.M. Mirsalimov, "The origin of a crack-type defect in the sleeve of a contact pair", Mathematical modeling, vol. 17, No. 2, pp. 35-45, 2005 Vestnik of Baku University. Physico-Math. Nauki, No. 3, 2015, pp. 128-133

Azerbaijan University of Architecture and Construction
ISSN 2706-7726
Engineering Mechanics
Scientific and Technical Journal
E-mail: engineeringmechanics@azmiu.edu.az

| September 2023 | Issue 14 | Volume 6 | Number 2 | Pages 34-36 |
|---|---|---|---|---|

# THE EFFECT OF TRANSMISSION ON SURFACE QUALITY DURING BALL ROLLING

**T.I. ASLANOV, M.V. NAGHIYEVA**
*Azerbaijan University of Architecture and Construction,*
aslanov1946@gmail.com, melahet.nagiyeva@gmail.com

**Abstract.** *The article is devoted to the issues of improving the quality of the top layers of various construction steels. This article uses ball rolling, a recently widely used surface plastic deformation method. It is known that longitudinal transmission is one of the parameters affecting the results of the ball rolling process (SH). Studies have shown that changing the value of transmission within a certain limit has a serious effect on the quality of the steel surface. Thus, the ball rolling process, carried out in optimal modes, reduced the roughness of the surface of the construction steels of the investigated point by several times and increased its hardness by an average of 25-45%. The decrease in surface roughness and increase in hardness leads to an increase in the operational properties of steel.*

**Keywords:** *structural steel, ball rolling, roughness, hardness.*

**Introduction**. The quality of the surface of machine parts and elements of structures depends on its geometric parameters and physico-mechanical properties. The quality of the surface has a significant impact on the working properties of the part - fatigue strength, corrosion resistance, contact fatigue resistance, corrosion resistance [1]. The optimum surface should have sufficient hardness, small structure, roughness with circular depressions and ridges, micro-smoothness with large bearing area and residual compressive stresses.

Commonly applied methods such as final processing methods (e.g. polishing, honing, handing, etc.) provide the part with the required shape and dimensions that ensure sufficient accuracy, but do not fully ensure the optimum quality of the surface.

In this respect, the surface-plastic deformation method is widely used to improve the surface quality of the part. Simpler and more effective methods of surface plastic deformation are ball rolling and diamond smoothing. As a result of machining the surface of the part with the specified methods, the roughness of the surface is reduced several times and the physical and mechanical properties (hardness, stress state, microstructure) are improved. It is therefore recommended to successfully use ball rolling or diamond smoothing methods instead of labor-intensive polishing and handing operations.

Plastic deformation is the main factor affecting the structural state of the upper layers of steel during ball rolling and diamond smoothing. Plastic deformation occurs as a result of the displacement of individual parts of the crystal along shear planes. In this case, the structure of the upper layers of steel is reduced and flexes in the direction of the acting force. Under the influence of plastic deformation, the phase composition of the upper layers of the metal changes. The amount of austenite remaining in the tempered steel after polishing can reach 30-40%. The presence of residual austenite in steel is undesirable because it has a negative effect on fatigue strength and corrosion resistance [5].

Surface plastic deformation methods greatly reduce the amount of residual austenite formed during the previous process [6].

The article investigates the effect of ball rolling, a surface-plastic deformation method, on the quality parameters of the surface of various structural steels.

**Discussions.** Comparative test experiments were conducted to study the effect of ball rolling on the surface roughness and hardness of 09ГС, 17Г2, 10ХСНD, 14Г2АФ and 14Х2ГМФ steels. The experiments were carried out using specimens of the specified steels with a diameter of 20 *mm* and a length of 120 *mm*. After polishing, the samples were subjected to thermal treatment. Then, one batch of specimens was prepared at a time with a ball with a diameter of 5 *mm*, a force of 800 *N* and a velocity of $V_H$=45 *m/min*. Longitudinal transmission is one of the parameters that significantly affects ball machining results. Therefore, studies have been carried out to reveal the effect of rolling on the surface quality of the examined structural steels.

The effect of yielding on the surface roughness of specimens made of 09ГС, 17Г2, 10ХСНD, 14Г2АФ and 14Х2ГМФ steels is shown in Figure 1.

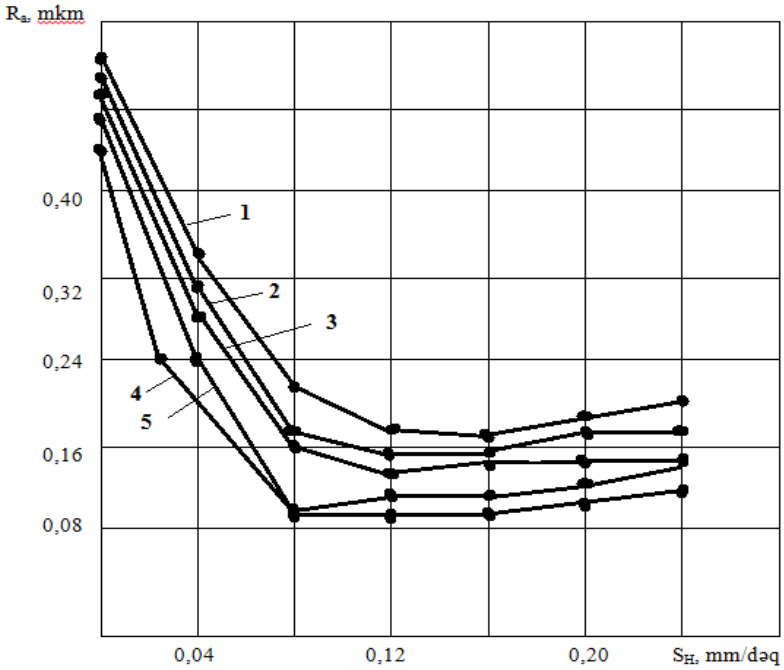


**Figure 1. Dependence on the roughness of the surface 1-09 ГС; 2-17Г2: 3-10ХСНD; 4-14Г2АФ: 5-14Х2ГМФ**

As can be seen from Figure 1, as the value of the transmission increases, the value of the roughness parameter Ra decreases and the minimum value of the roughness is achieved at values of approximately $S_H$=0.08-0.16 *mm/rev.* Further increase in transmission leads to deterioration of the surfaceroughness.

The effect of transmission on the hardness of the structural steels examined is shown in Figure 2.

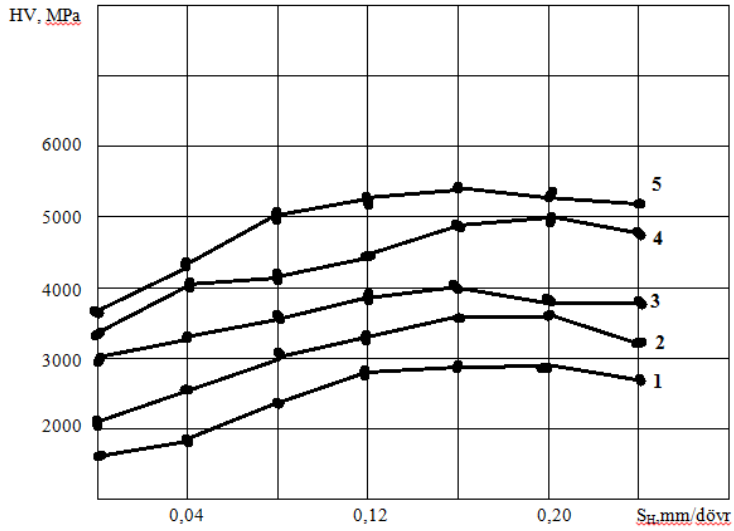


**Figure 2. Dependence of surface hardness on transmission**
**1-09 ГС; 2-17Г2: 3-10ХСНD; 4-14Г2АФ: 5-14Х2ГМФ**

As can be seen from the graphs, the maximum hardness of all steels is achieved at $S_H$=0.12-0.16 *mm/rev*. The subsequent transmission increase leads to a reduction in the surface hardness of the steels.

**Conclusion**. The test experiments show that the optimal value of the ball rolling process should be adopted as $S_н$=0.08-0.16 *mm/rev* to improve the surface quality of the examined construction steels. At transmission value below 0.08 *mm/rev*, the surface roughness and hardness change very little due to the excessive knocking of the steel surface.

At transmission values above 0.16 *mm/rev*, there is an increase in roughness and a decrease in hardness, i.e. deterioration in the quality of the steel surface. Therefore, in order to improve the quality of the upper layers of the studied steels 09ГС, 17Г2, 10ХСНД, 14Г2АФ and 14Х2ГМФ, the value of the ball rolling process should be taken as 0.12-0.16 *mm/rev*.

## References

1. Boitsov, V.B. Technological methods for increasing strength and durability / V.B.Boitsov, A.O. Chernyavsky. - Moscow: Mechanical Engineering, -2005. - 127 p.
2. Gamzaeva, G.R. The influence of feed and number of passes during diamond burnishing on roughness // - Dnipro: Problems of computational mechanics and value of structures, - 2022. №. 34, - p. 16-22.
3. Ezhelev, A.V. Analysis of methods for processing surface-plastic deformation / A.V. Ezhelev, I.N. Bobrovsky, A.A. Lukyanov // - Moscow: Fundamental Research, -2012. № 6-3, - p. 642-646
4. Kochetkov, A.V. Review of studies of finishing-hardening processing methods of surface plastic deformation / A.V. Kochetkov, F.Ya.Barats, I.G. Shashkov // - Moscow: Science Studies, -2013. №. 4, - p. 1-19.
5. Mammadov. A.T. About the effect of surface-plastic deformation parameters on surface hardness / A.T. Mammadov, T.I. Aslanov, G.R. Ganzayeva //-Baku: Scientific works of AzTU, -2018. №3, - p.27-32

Azerbaijan University of Architecture and Construction
ISSN 2706-7726
Engineering Mechanics
Scientific and Technical Journal
E-mail: engineeringmechanics@azmiu.edu.az

| September 2023 | Issue 14 | Volume 6 | Number 2 | Pages 37-40 |
|---|---|---|---|---|

# ANALYTICAL STUDY OF THE EFFECT OF POROSITY ON THE MECHANICAL PROPERTIES OF THE MATERIAL

**O. Y. EFENDIEV**
*Azerbaijan University of Architecture and Construction*
o.efendiyev@mail.ru

**Abstract.** *When porous bodies come into contact with liquids, liquids penetrate into them, as a result of which they turn into a two-phase medium. When we talk about liquids, we mean both liquids and gases. True liquids will be treated as liquids with a small compression, and gases as liquids with a large compression. The rest of the body, except for the pores, we will call the skeleton. The pores in the bodies communicate with each other through capillary tubes. Under the influence of external forces, the skeleton of a porous body is deformed, and over time the volume of pores changes, which leads to a change in the specific mass of the liquid in its body. Below we will prove that the physical properties of a porous material depend on the specific mass of the liquid in its pores.*

**Keywords:** *porous bodies, capillary tubes, skeleton, Jung module.*

## I. INTRODUCTİON

Thus, the change in the volume of pores over time leads to the formation of deformations, which are a function of time. When such deformations are reversible (at small stresses), they are called core-elastic deformations. Now let's take formulas for The brought physical properties of two-phase media. Let's accept the following markup.

Volume of a porous body -V;
Volume of the skeleton -$V_s$;
Volume of fluid in the pores -$V_m$;
Mass of the skeleton - $m_s$;
The mass of a body whose pores are filled with liquid -*m*;
Mass of liquid in pores - $m_m$;
Density of the skeleton - $\rho_s$;
Density of a body whose pores are filled with liquid – ρ;
Density of fluid in pores - $\rho_m$.

## II. SOLUTION OF THE ISSUE

Among these nine quantities are the following dependencies.

$$m_m = m - m_s ; \quad (1)$$

$$Vm = \frac{m-m_s}{\rho_m} ; \quad (2)$$

$$V_s = V - V_m = V - \frac{m-m_s}{\rho_m} ; \quad (3)$$

(1) from

$$\rho_s = \frac{m_s}{V_s} = \frac{m_s}{V-V_m} ; \quad (4)$$

$$m_m+m_s= m;$$

from here

$$\frac{m_m}{m}+\frac{m_s}{m}=1. \quad (5)$$

Now let's get an expression for The brought Jung module of a body whose pores are filled with liquid. As the law of law in uniaxial traction is known

$$\varepsilon=\frac{\sigma}{E}, \quad (6)$$

in shape. Where e is the Yung modulus, σ is the tensile stress, ε is the relative elongation. (6) from

$$E_s=\frac{F}{\frac{m_s}{m}\cdot S\cdot\varepsilon}=\frac{m}{m_s}\cdot\frac{F}{S\cdot\varepsilon}=\frac{m}{m_s}\cdot E\,. \quad (8)$$

Thus, the Yung module of the skeleton is different in M/m_s times from the Yung module $\frac{m}{m_s}$ of the body, which has filled the pores with liquid.

When compressing the rod, the compressive deformations of the fluid column in its skeleton and pores are equal to each other, i.e. $\varepsilon_s=\varepsilon_m$

$$\frac{T_s}{S_s\cdot E_s}=\frac{T_m}{S_m\cdot E_m} \quad (9)$$

Here, the cross to Ts and Tm-is –section according the compressive forces acting on the skeletal and pore sections, $S_s$, $E_s$ and $S_m$, $E_m$, the cross-section area of the skeleton and fluid according to Em, and the Jung module. On the other hand, the compressions of both the skeleton and the liquid column and the common element are equal to each other, that is

$$\frac{T_s}{S_sE_s}=\frac{T_m}{S_m\cdot E_m}=\frac{T_s+T_m}{(S_s+S_m)E_g}$$

Here is the EG- $E_g$ brought yung module. From the last equality

$$E_g=\frac{m_sE_s+M_mE_m}{M} \quad (10)$$

For the Poisson coefficient- $v_g$, flow rate - $\sigma_g$, brought by the analogous rule, the following expressions can be obtained.

$$V_g=\frac{m_sV_s+m_mV_m}{m}; \quad (11)$$

$$\sigma_g=\frac{m_s\sigma_{sa}+m_m\cdot\sigma_{ma}}{m}; \quad (12)$$

(10) - (12) bərabərliklərində *s* indeksli kəmiyyətlər skeletə, *m* indeksli kəmiyyətlər isə mayeyə aiddirlər (10) bərabərliyində $m=m_s+m_m$ olduğunu nəzərə alsaq $E_g$ üçün alarıq.

$$E_g=\frac{m_sE_s+m_mE_m}{(m_s+m_m)^2}\,. \quad (13)$$

Since the time of deformation changes little by little the volume of the skeleton and the volume of the pores changes a lot, in (13) we look at $m_m$ as a variable quantity and take the derivative from Eg by $m_m$

$$E_g^1 = \frac{m_s(E_m - E_s)}{(m_s + m_m)^2}, \quad (14)$$

it is possible. As can be seen from (14), $E_m > E_s$ . is positive when Em>Es, and $E_g^1$. is negative when Em<Es. This means that regardless of the mass of liquids in the pores, if the Yung modulus of the liquid is greater than the Yung modulus of the skeleton, the Yung modulus brought increases when the mass of the liquid increases, but if the Yung modulus of the liquid is less than that of the skeleton, it decreases if we build a graph 1.)

If the fluid in the pores of the object is incompressible, it becomes $v_m$=0.5. In this case (11) from

$$v_g^1 = \frac{m_s(0{,}5 - V_s)}{(m_s + m_m)^2}. \quad (15)$$

It is known that for any material $0 \le v \le 0.5$. Always $v_g^1 \ge 0$ when the pores are filled with incompressible fluid, as can be seen from (15). And this means that the Poisson coefficient of a body filled with liquid, the pores of which are not compressed, always increases as the fluid in the pores increases. graph of dependence of vg on mm figure 2.it happens like in.

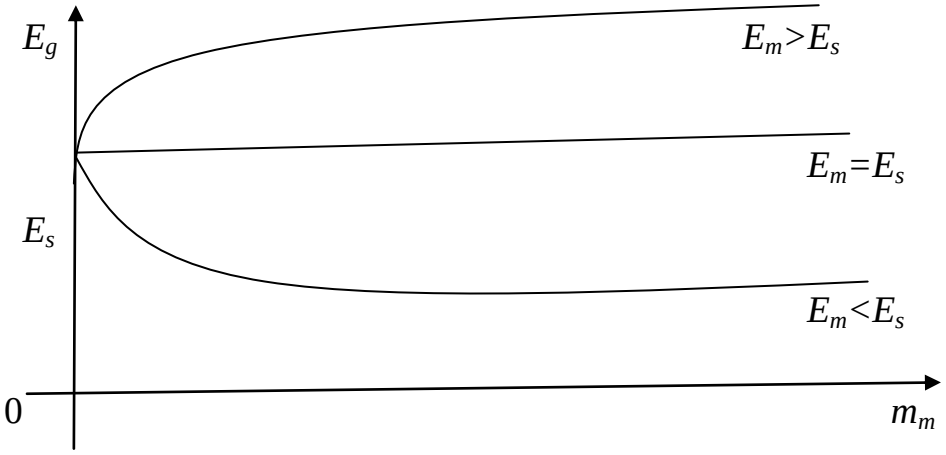


Fiqure 1. From the mass of liquid in the pores of The brought Jung module addiction timeline

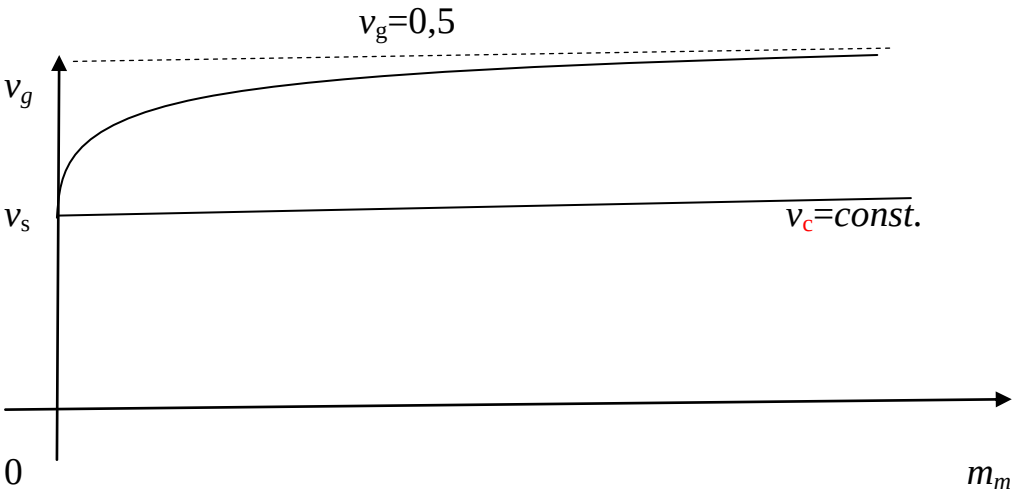


Figure 2. Graph of the dependence of The brought Poisson coefficient on the mass of the liquid in the pores.

**Results**

1. Expressions have been obtained for mechanical characteristics of bodies whose pores are filled with liquid.

2. It has been theoretically proven that when the Yung modulus of the fluid in the pores is larger than that of the skeleton, The introduced yung modulus increases as the mass of the fluid increases, and vice versa when the Yung modulus of the fluid is smaller than that of the skeleton, it decreases as the mass of the fluid increases.
3. When the pores are filled with incompressible liquid, the Poisson coefficient always increases as the mass of the liquid increases, that is, a state of decrease is impossible.

## REFERENCES

1. Alizade A.N., Gulgazli A.S., Hasanov A.I. Generalization of one variational principle taking into account the effect of neutron irradiation on the creep of the material. Izv.AN Azerbaijan SSR. A series of physics and mathematics. Sciences, 1985, No. 4, pp. 49-52.
2. Alizade A.N., Gulgazli A.S. Variational principle for determining the stress-strain state of an elastic shell under irradiation, taking into account geometric nonlinearity Izv.AN of the Azerbaijan SSR. A series of physics and mathematics. Sciences, 1979, No.6, pp. 84-87.
3. Gülgəzli Ə.S., Əfəndiyev O.Y. İki tərəfdən oynaqlı bərkidilmiş məsaməli-lövhənin şişmədən dayanıqlıq qabiliyyətinin itirilməsi. ISSN 2409-4560 AzİMETİ Azərbaycanda Inşaat və Memarlıq 3 (18) 2018.
4. Hajiyev V.D. On deformation and stability of viscoplastic structural elements in the presence of initial stresses. The All-Union. conf. on composite materials. Tez. dokl. Yerevan, 1987, vol. 2. pp. 68-70.
5. Hasanov R.A., Gulgazli A.S., Zeynalov A. And the general view of the equation of state of the porous medium Azerbaijani Oil Industry, No.9,2016, pp.31-33.
6. Hasanov R.A., Shirali I.Ya., Medzhidov G.N., Pirmamedov I.T., Gulgazli A.S. Solution of mechanical and mathematical models of drilling processes. AGNA Publishing House .Baku-2010.340 p.

Azerbaijan University of Architecture and Construction
ISSN 2706-7726
Engineering Mechanics
Scientific and Technical Journal
E-mail: engineeringmechanics@azmiu.edu.az

| September 2023 | Issue 14 | Volume 6 | Number 2 | Pages 41-45 |
|---|---|---|---|---|

# VIBRATIONS OF FUNCTIONALLY-GRADED CYLINDRICAL SHELL CONTACTING A VISCO-ELASTIC LIQUID

**DAVUD HÜSEYNI KAKLAR**
*Azerbaijan Architecture and Construction University*
davoud_h_k@yahoo.com

**Abstract**-*Functional-gradient coverings find applications in a variety of engineering structures such as aircraft, spacecraft, rockets, automobiles, computers, underwater and surface vessels, bridges, and building roofs. The continuous advancement in material science and engineering, coupled with the increasing demand for flexible constructions, has led to the utilization of modern materials, including layered composites and functional gradient materials (FGMs), in the design of shell structures. Among various applications, aerospace and aeronavigation applications are particularly challenging due to their intricate interactions of shell structures and the use of novel materials with less well-known properties.*

**Keywords**: *Functional-gradient material, layered composites, visco-elastic environment, Navier-Stokes equation, Hamilton-Ostrogradsky effect.*

## I. INTRODUCTION

The problems related to the vibrations and durability of coverings made from functional-gradient materials have been addressed in various studies [1-6]. Some works [7-9] focused on the non-linear behavior of a rectangular plate made from functional-gradient material, while others [10, 11] investigated the linear vibrations of a functional-gradient covering. The non-linear vibrations of a functional-gradient cylindrical covering in contact with moving fluid under various reinforcement conditions were studied in [12, 13, 14]. The variational principle of Hamilton-Ostrogradsky was employed to determine the equations of motion, and the motion equations of the solved differential equations system were solved by conventional methods. The motion equation of the visco-elastic material was formulated using the vector equation of the Navier-Stokes equation.

This paper is dedicated to the non-linear vibrations of a functionally-graded cylindrical covering with various forms of reinforcement in contact with moving fluid.

## II. PROBLEM FORMULATION.

The effective physical and mechanical characteristics of materials made from functional-gradient materials depend on the material's P-properties and volume V. The efficiency coefficient of two coverings made from functional-gradient materials is calculated by the formula:

$$P_{eff} = P_1V_1 + P_2V_2 \qquad (1)$$

Here, E represents the elastic modulus, ν represents the Poisson's ratio, and ρ represents the density.

Consider a cylindrical shell composed of a mixture of ceramic and metal in contact with the fluid (Figure 1).

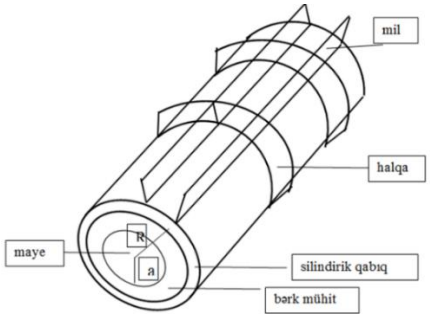


Figure 1. Functional-gradient cylindrical shell with rings reinforced, undergoing fluid motion in the channel.

As calculated in the work [10], the volume fractions are determined by the laws: [8, 9, 10]

$$V_1 = \left(\frac{2z+h}{2h}\right)^k, \quad V_2 = 1 - V_1 \qquad (2)$$

Here, h represents the thickness of the coating, and k is the power exponent of the ceramic material's volume fraction, with $0 \le k \le \infty$. If k=0, the structure of the coating consists only of ceramics, and if $k=\infty$, it will be entirely composed of metal. The mechanical properties of the composite, consisting of two components, including Young's modulus, Poisson's ratio, density, and , are calculated by the following rules:

$$P_{eff} = (P_c - P_m)\left(\frac{z}{h} + \frac{1}{2}\right)^k + P_m \qquad (3)$$

Using the principle of (3), it is possible to calculate the elastic modulus E, Poisson's ratio ν, and density ρ of the composite. Here, $P_c$ and $P_m$ are the characteristics of the ceramic and metal, respectively. The motion equations of the composite cylindrical shell in contact with the environment are determined based on the Hamilton-Ostrogradsky variational principle [11,12,14].

$$\delta W = 0 \qquad (4)$$

Here, $W = \int_{t'}^{t''} L dt$ – represents the Hamiltonian action, where $L = K - \Pi$ is the Lagrangian function, and $t'$ and $t''$ are arbitrary instants in time.

The potential and kinetic energies of the functional-gradient cylindrical shell are expressed as follows:

$$U = \frac{1}{2}\iint_\Omega (N_{11}\varepsilon_{11} + N_{22}\varepsilon_{22} + N_{12}\varepsilon_{12} + + M_{11}\chi_{11} + M_{22}\chi_{22} + M_{12}\chi_{12})\, d\Omega +$$

$$+ \frac{1}{2}\iint_\Omega \left(Q_x(w_{,x} + \psi_x) + Q_y(w_{,y} + \psi_y)\right) d\Omega \qquad (5)$$

$$T = \frac{1}{2}\iint_\Omega I_0(u_{,t}^2 + v_{,t}^2 + w_{,t}^2) + 2I_1(u_{,t}\psi_{x,t} + v_{,t}\psi_{y,t}) + I_2(\psi_{x,t}^2 + \psi_{y,t}^2)\, dxdy \qquad (6)$$

Here, $I_0 = \left(\rho_m + \frac{\rho_c - \rho_m}{k+1}\right)h$, $I_1 = \int_{-\frac{h}{2}}^{\frac{h}{2}} \rho(z) z dz = \frac{(\rho_c - \rho_m)k}{2(k+1)(k+2)}h^2$,

$$I_2 = \int_{-\frac{h}{2}}^{\frac{h}{2}} \rho(z) z^2 dz = [\frac{\rho_m}{12} + (\rho_c - \rho_m)(\frac{1}{k+3} - \frac{1}{k+2} + \frac{1}{4(k+4)})]h^3$$

The work done by the pressure force exerted by the fluid on the functional-gradient shell due to its displacement on the fluid side is calculated as follows: $A_0 = -\iint_\Omega p w dx dy$

The terms involved in the expressions for the potential and kinetic energies of the functional-gradient cylindrical shell, as given in equation (5), are:

$$\varepsilon_{ij} = \varepsilon_{ij}^{L} + \varepsilon_{ij}^{ND}, \quad \mathbf{(i,j=1,2)}, \ \varepsilon_{11}^{L} = u_{,x} + w/R_x, \ \varepsilon_{22}^{L} = v_{,y} + w/R_y, \varepsilon_{12}^{L} = u_{,y} + v_{,x}$$

$$\varepsilon_{11}^{ND} = \frac{1}{2}w_{,x}^{2}, \ \varepsilon_{22}^{ND} = \frac{1}{2}w_{,y}^{2}, \ \varepsilon_{12}^{ND} = w_{,x} + w_{,y}, \ \varepsilon_{13} = w_{,x} + \psi_x, \ \varepsilon_{23} = w_{,y} + \psi_y,$$

$$\varepsilon_{11}^{ND} = \frac{1}{2}w_{,x}^{2}, \ \varepsilon_{22}^{ND} = \frac{1}{2}w_{,y}^{2}, \ \varepsilon_{12}^{ND} = w_{,x} + w_{,y}, \ N = \{N_{11}; N_{22}; N_{12}\}^{T} = \frac{1}{1-\nu^2}[C](E_1\varepsilon + E_2\chi),$$

$$M = \{M_{11}; M_{22}; M_{12}\}^{T} = \frac{1}{1-\nu^2}[C](E_2\varepsilon + E_3\chi), \ E_1 = \left(E_m + \frac{E_c - E_m}{k+1}\right)h, \ \mathrm{E}_2 = \frac{(E_c - E_m)kh^2}{2(k+1)(k+2)},$$

$$E_3 = \left(\frac{E_m}{12} + (E_c - E_m)\left(\frac{1}{k+3} - \frac{1}{k+2} + \frac{1}{4(k+4)}\right)\right)h^3, \ \rho = \left(\rho_m + \frac{\rho_c - \rho_m}{k+1}\right)h,$$

The cutting forces $Q_x$ and $Q_y$ are determined from the expressions $Q_x = K_S^2 A_{33}\varepsilon_{13}, \ Q_y = K_S^2 A_{33}\varepsilon_{23},$ where $K_S^2$ is referred to as the regulator coefficient. In the calculation process, $K_S^2$ is assumed to be $\frac{5}{6}$. $A_0$ – represents the pressure force exerted by the fluid on the shell, and the work done by this force on the displacement of the shell *w* is negative. The pressure force $p$ is determined from the motion equation of the ideal fluid moving with velocity $U$ :

$$\Delta\tilde{\varphi} - \frac{1}{a_0^2}\left(\frac{\partial^2\tilde{\varphi}}{\partial t^2} + 2U\frac{\partial^2\tilde{\varphi}}{R\partial\xi\partial t} + U^2\frac{\partial^2\tilde{\varphi}}{R^2\partial\xi^2}\right) = 0 \qquad (6)$$

At the contact of the overlaying fluid, equality of velocity and pressure in the radial direction is satisfied:

$$\vartheta_r\big|_{r=R} = \left.\frac{\partial\tilde{\varphi}}{\partial r}\right|_{r=R} = -\left(\omega_0\frac{\partial w}{\partial t_1} + U\frac{\partial w}{R\partial\xi}\right), \quad q_z = -p_{|r=R} \qquad (7)$$

Seeking the potential $\tilde{\varphi}$ of excitations as follows:

$$\tilde{\varphi}(\xi, r, \theta, t_1) = f(r)\cos n\theta \sin kx \sin \omega t \qquad (8)$$

Here, $n, k$ – are the wave numbers in the coordinate axes direction, $\omega$ – is the unknown frequency, and $f(r)$ – is an unknown function. Using expressions (7), (8), and (9), we obtain:

$$\tilde{\varphi} = -\Phi_{\alpha n}\left(\omega_0\frac{\partial w}{\partial t_1} + U\frac{\partial w}{R\partial\xi}\right), \ p = \Phi_{\alpha n}^{*}\rho_j\left(\omega_0^2\frac{\partial^2 w}{\partial t_1^2} + 2U\omega_0\frac{\partial^2 w}{R\partial\xi\partial t_1} + U^2\frac{\partial^2 w}{R^2\partial\xi^2}\right). \qquad (9)$$

As a result, for the fully reinforced cylindrical shell in contact with a moving fluid, we consider the total energy of the functional-gradient shell:

$$L = U + T + A_0 + \sum_{i=1}^{k_1}(\Pi_i + K_i) + \sum_{j=1}^{k_2}(\Pi_j + K_j)\cdot \qquad (10)$$

It is considered that at $x = 0$ and $x = L$ cuts, the following conditions are satisfied:

$$u = 0, \ \mathrm{w}=0, \ \mathrm{T}_1 = 0, \ M_1 = 0 \qquad (11)$$

Thus, the solution to the problem of non-linear vibrations of the functional-gradient cylindrical shell in dynamic contact with the fluid involves the integration of the total energy of the construction (13), which consists of the functional-gradient cylindrical shell filled with the fluid in the internal region.

**SOLUTİON OF THE PROBLEM.**

The expression for the determined pressure p, based on equation (5), is given as follows:

$$p = p_0 J_n(\lambda r) e^{i(kx+n\theta+\omega t)} \qquad (12)$$

If we substitute this expression into the Navier-Stokes equation (6) and apply the method of variation of constants using the expressions $\varphi = \varphi_*(r) e^{i(kx+n\theta+\omega t)}$, we obtain the following for $\varphi$ to determine the functions $\varphi$ and $\bar{\psi}$: $\Delta\varphi = -\frac{1}{a^2\rho_0}\frac{\partial p}{\partial t}$; $\Delta\bar{\psi} = \frac{1}{\bar{\mu}}\frac{\partial\bar{\psi}}{\partial t}$.

$$\varphi = \left(\frac{i\omega}{a^2\rho_0} p_0 f(r) + \mu_1 J_n(kr)\right) e^{i(kx+n\theta+\omega t)}. \qquad (13)$$

Searching for the displacements of the covering as follows:

$$u = u_0 e^{i(kx+n\theta+\omega t)}; \vartheta = \vartheta_0 e^{i(kx+n\theta+\omega t)}; w = w_0 e^{i(kx+n\theta+\omega t)}. \qquad (14)$$

Here, $u_0, \vartheta_0, w_0$ are unknown constants, while $\chi, n -$ are the wave numbers in the radial and azimuthal directions of the cylindrical shell, respectively.

In the context of the Hamilton-Ostrogradski determination condition, we obtain a system of second-order partial differential equations for the unknown constants $u_0, \vartheta_0, w_0$. Considering the variations with respect to $u_0, \vartheta_0, w_0$, and setting the coefficients of non-dependent variations to zero, we derive a system of coupled equations. By setting the determinant of this system to zero, we obtain the eigenfrequencies for the cylindrical shell in dynamic contact with a self-elastic medium.

$$\det\left\|a_{ij}\right\| = 0, \quad \text{i,j=1,2,3} \qquad (15)$$

Equation (15) has been computed using the variational method.

## III. CONCLUSIONS

The following values were taken for the parameters in the calculation:

$\rho_0 / \rho = 0{,}115$; $E_m / E_c = 70/380$; $\nu_m = \nu_c = 0.3$; $\rho_m = \rho_c = 2707$; $a_0 = 1350$ m/sec, $\bar{\mu}$=0.355

In Figure 1, the dependence of the axial velocity parameter on the volume fraction exponent $k -$ of the ceramic material is presented. As the volume fraction exponent of the ceramic $k$ material increases, the system's axial vibration frequencies decrease, as shown in Figure 1. $\Omega_x = \omega h\sqrt{\rho_c / E_c}$

The graph shows the cases where the density of the fluid is considered in curve 1 and where it is not considered in curve 2. As seen, considering the density of the fluid leads to a decrease in the system's specific vibration frequencies.

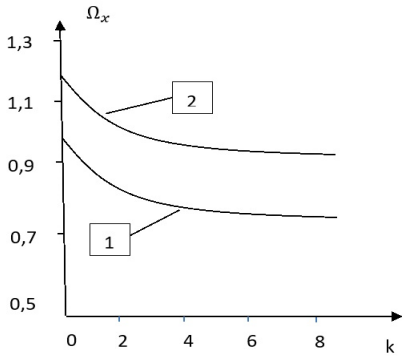


Figure 2. Dependence of the system's vibration frequencies on the volume fraction exponent.

## REFERENCES

1. Alijani F. , Amabili M., Karagiozis K., Bakhrtiari-Nejad F. Nonlinear vibrations of functionally graded doubly curved shallow shells // Journal of Sound and Vibration. - 2011. – 330. – P.1432 – 1454.
2. J.N. Reddy, Loy C.T., Lam K.Y., Vibration of functionally graded cylindrical shells // Int J Mech Sci. – 1999. – 41. – P.309 – 324.
3. Matsunaga H. Free vibration and stability of functionally graded shallow shells according to a 2D higher-order deformation theory // Composite Structures. – 2008. – 84. – P. 132 – 146.
4. Reddy J.N. Analysis of functionally graded plates // International Journal for numerical methods in engineering. – 2000. – 47. – P. 663 – 684.
5. Shen H.S. Functionally Graded Materials of Plates Shells / Florida: CPC Press, 2009. – 266p.
6. Chorfi S.M., Houmat A. Non-linear free vibration of a functionally graded doubly-curved shallow shell of elliptical plan-form // Composite Structures. – 2010. – 92. – P. 2573 – 2581.
7. L.V.Kurpa, T.V.Shmatko Investigation of geometrically nonlinear oscillations of functionally gradient flat shells with a complex plan shape//Bulletin of the Zaporozhye National University.- 2015, No.1. pp.89-97.
8. Kurpa L.V. Nonlinear free oscillations of multilayer flat clouds of symmetrical structure with a complex plan shape // Mat. Methodi ta fiz. – fur. fields. – 2008. – 51 , №2. – Pp. 75-85.
9. Kurpa L.V. The R - function method for solving linear problems of bending and oscillation of flat areas/ Kharkiv: NTU "KhPI" , 2009. – 408 p.
10. Kurpa L.V. Shmatko T.V. Free oscillations of functionally gradient flat shells with a complex plan shape // Theory. and applied mechanics. - 2014. – Issue 8(54). – pp. 77-85.
11.Iskanderov R.A., Hosseini Kaklar D. Geometrical nonlinear vibrations of a moving shellfluid-contacting functionally graded cylindrical Problems of computational mechanics and strength of structures, Dnepropetrovsk National University named after Oles Honchar, vol.26 , 168-174 , 2017
12. Iskanderov R.A., Hosseini Kaklar D. Geometrical nonlinear vibration of functionally –graded longitudinally strengthened and flowing fluid –contacting cylindrical shell. IJTPE Journal International Journal on Technical and physical problems of engineering. Issue 32 Volume 9 Number 3 September pp. 44-52, 2017.
13.Rvachev V.L. Theory of the R-function and some of its applications / Sciences. Dumka, 1982. - 552 p.
14. Hossein Kaklar D.Sh. Oscillations of a functional-gradient silimdric shell reinforced with longitudinal ribs, interacting with a viscous-elastic fluid.Ecology and water economy, №4, p. 75-80, 2019.

Azerbaijan University of Architecture and Construction
ISSN 2706-7726
Engineering Mechanics
Scientific and Technical Journal
E-mail: engineeringmechanics@azmiu.edu.az

| September 2023 | Issue 14 | Volume 6 | Number 2 | Pages 46-50 |
|---|---|---|---|---|

# NUMERICAL MODELING OF BURIED SEWER PIPELINE USING PLAXIS SOFTWARE

**Tural Rustamli**

rustamli.tural.90@gmail.com

**Abstract-** *The paper studies the stress-strain state of underground fiber-reinforced concrete pipes. As the diameter of the pipes increases, the lateral effect of seismic load on the surface of the pipeline increases. The adopted pipeline model with different stiffness (longitudinal, transverse and vertical) simulates the connection of the pipeline with the surrounding soil. The equation for the dynamic behavior of the pipeline under seismic influence was solved using the Plaxis software. The compiled stiffness matrices and mass matrix were included in the solution of the general equation. The results of the numerical solution for determining tensile and compressive stresses are presented in tabular form.*

***Keywords:*** *fiber concrete, pipe, stress, strength, stiffness, tension*

## 1. INTRODUCTION

One of the urgent tasks at the present stage is to increase the safety of underground pipeline communication objects. High vulnerability to intense natural impacts requires special approaches to design, construction and operation in seismic zones.

Currently, the calculation for resistance to seismic impact for underground pipelines is carried out only on the basis of the longitudinal loads from the seismic waves, whereas the lateral loads are neglected. For large magnitude earthquakes this approach to strength calculations is not fully correct in view of the probable damage to the pipe from the additional hoop stress [8].

The evaluation and accounting of the lateral seismic loads contribution to the overall stress-strain state of underground pipelines is an important engineering problem, which has great practical significance for improving the safety of extended underground pipeline.

## 2. TWO-DIMENSIONAL MODEL FOR CALCULATING AN UNDERGROUND PIPELINE FOR SEISMIC IMPACT

During an earthquake, due to the action of a seismic force transverse to the longitudinal axis, the pipeline is displaced along the Y axis under the influence of the upper influence of the soil and the sediment of the liquefied soil settles along the Z axis. To study the bending of pipelines in a two-dimensional model in the design scheme, the connection of the pipeline with the soil is replaced by a system of springs. The differential equation of the underground pipe model can be written [4, p.121]

$$M_0(\ddot{u_r}) + \psi(u_r) + K(u_r) = -M_0(\ddot{u_0}) \quad (1)$$

where $M_0 = M_b + M_{gr}$ - common mass of the "pipeline+ground" systems; $M_b$ - mass of pipe; $M_{gr}$ - added ground mass ($M_{gr} \approx 0{,}5M_b$) ; $u_r$ , $\dot{u_r}$ , $\ddot{u_r}$ - respectively displacement, velocity and acceleration; $K$ - elastic coefficient during pipe displacement ; $\ddot{u_0}$ - received seismic wave acceleration. In matrix form may to write as [4, p.121]

$$[M]\{\ddot{u}\} + [\psi]\{\dot{u}\} + [K]\{u\} = [M]\{\ddot{u}_0\} \quad (2)$$

where $[K], [M]$ – stiffness and mass matrix of pipe [7];

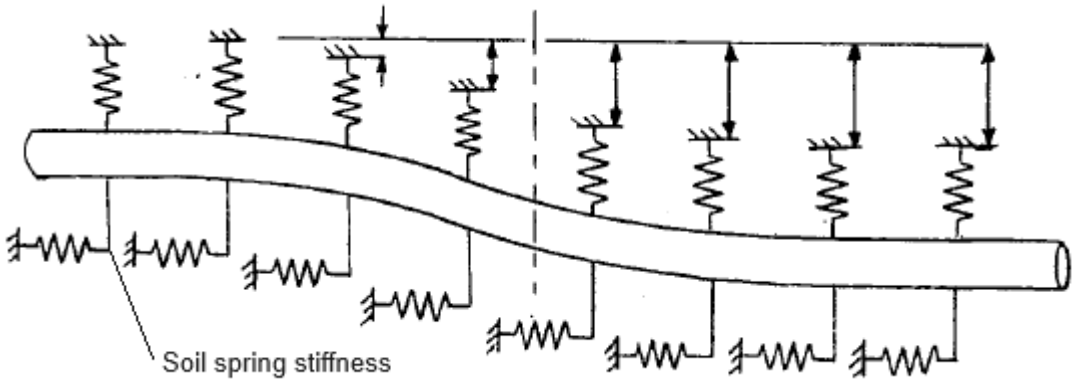


**Fig. 1.** Design scheme of the soil massif around the pipeline

$[u], [\dot{u}], [\ddot{u}]$ - respectively displacement, velocity and acceleration matrix; $[\ddot{u}_0]$ - received seismic wave acceleration matrix.

Normal and shear stress in the "pipe + soil" system are interconnected [4, 7]:

$$\begin{Bmatrix} \sigma_n \\ \tau \end{Bmatrix} = \begin{bmatrix} K_n & K_{ns} \\ K_{sn} & K_s \end{bmatrix} \begin{Bmatrix} u_n \\ u_s \end{Bmatrix} \quad (3)$$

where $u_n$ - normal lateral displacement; $u_s$ - longitudinal sliding movement; $K_{ns}$ and $K_{sn}$ -stiffness between normal and sliding displacements. Normal and slidding stiffness may to write as [8]:

$$K_n = \frac{E(1-\mu)}{(1+\mu)(1-2\mu)} \quad (4)$$

$$K_s = \frac{E}{2(1+\mu)} \quad (5)$$

where $E$ and $\mu$ -elastic modulus and Poisson ratio of composit fiber concrete matherial, whish defined from tests. Mass matrix defined as [4, p.121]

$$M = \begin{bmatrix} M_{11} & M_{12} \\ M_{21} & M_{22} \end{bmatrix} \quad (6)$$

The elements of this matrix include the density of the material (fiber-reinforced concrete), the cross-sectional area of the pipe, the lengths of the elements, the moment of inertia of the pipe section. For each nodal element, the mass matrix can be written as

$$[M_i] = \begin{bmatrix} m_i & 0 & 0 & 0 & 0 & 0 \\ 0 & m_i & 0 & 0 & 0 & 0 \\ 0 & 0 & m_i & 0 & 0 & 0 \\ 0 & 0 & 0 & I_{xxi} & -I_{xyi} & -I_{xzi} \\ 0 & 0 & 0 & -I_{yxi} & I_{yxi} & -I_{yzi} \\ 0 & 0 & 0 & -I_{zxi} & -I_{zui} & I_{zzi} \end{bmatrix} \quad (7)$$

The connection of the pipeline with the soil is modeled using lumped masses. At this time, the concentrated masses are expressed as the final nodal element $\boldsymbol{m_i}$ and the moments of inertia as $I_{xxi}$ , $I_{xyi}$, $I_{xzi}$, $I_{yxi}$, $I_{yxi}$, $I_{yzi}$, $I_{zxi}$ , $I_{zui}$ , $I_{zzi}$.

## 3. NUMERICAL MODELING OF THE STRESS STATE OF PIPE IN THE 2D SYSTEMS

The underground pipeline and the soil massif surrounding it is accepted as a uniform object. The soil massif around the pipeline is modelled by means of **PLAXIS 2D** software according to the square and diagonal scheme on a rectangular site (fig. 1). The external circle marked in green in the figure shows the contact element (interface) of the interaction of the structure with the soil. Properties of this massif is characterized by two constants - the module of elasticity of soil and Poisson's ratio. The geometrical change of the system (pipeline and soil massif) is associated with a change in mesh points. The cross contour of a pipe is also divided into finite elements. Pipe material (fiber concrete) is characterized by the module of elasticity and Poisson's ratio. **PLAXIS 2D** is a powerful finite element software package intended for calculation of the stress-strain state condition of structures, foundations and bases. Calculation was made in the conditions of plane deformation. In the calculation 15 nodal elements were used. In the study of the effective stresses arising in the

pipe the weight of backfill over the pipe, loads from a roadbed and dynamic loads from transport were considered together with the seismic influence. Stresses were calculated separately for the case of a reinforced concrete and fiber concrete pipe with a steel and polypropylene fiber (fig. 2 a, b). The similar procedure was carried out to determine the displacement of the pipe from the combination of acting vertical loads together with seismic loads. In the calculation, 2 layers of continental soil with a total height of 50 m with a crushed stone base 10 cm thick under the base of the pipe were taken. Under the influence of seismic force and the top of the underlying soil, the pipeline has horizontal ($u_x$) and vertical ($u_y$) displacement. For a pipe with a diameter of 3 m when exposed to seismic force, the horizontal displacement is $u_x$=35cm, $u_y$=10cm. Seismic acceleration was accepted 0.3g.

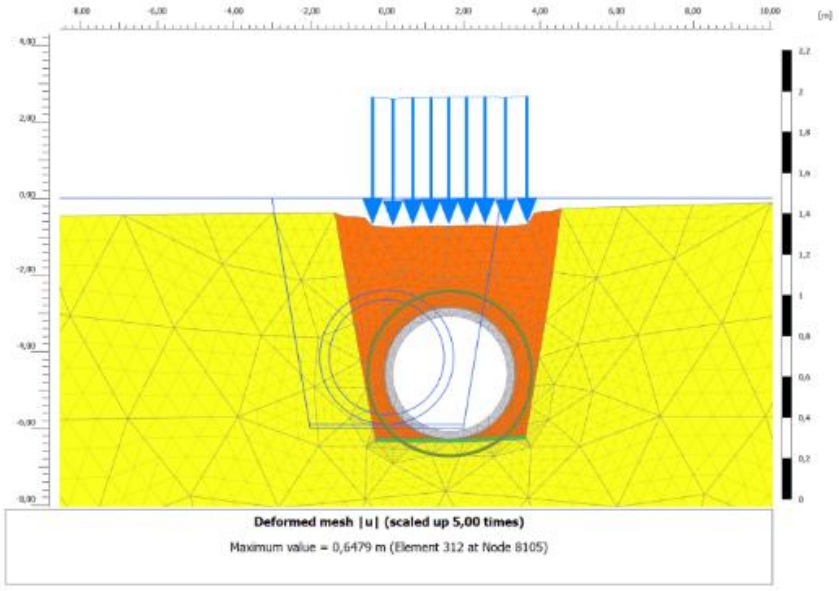


**Fig. 2.** Design scheme of the soil massif around the pipeline modelled by means of PLAXIS 2D

*a)* *b)*

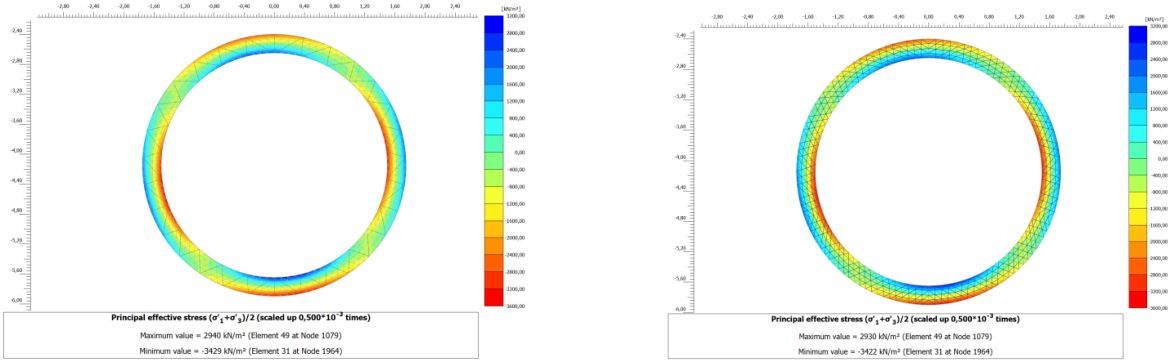


**Fig. 3.** Contour plots of the main effective stresses arising in the pipe section from a combination of seismic loads: a) reinforced concrete pipe; b) fiber concrete pipe with a metal fiber

## 4. THREE-DIMENSIONAL MODEL FOR CALCULATING AN UNDERGROUND PIPELINE FOR SEISMIC IMPACT

In the 3D system, the pipe model and ground connection is modeled as a system of springs in three directions with different stiffness's [5]. In matrix form, the stiffness matrix is written as the longitudinal stiffness matrix [4, p.121]

$$[K_{p,axial}] = \begin{bmatrix} \frac{EA}{L} & -\frac{EA}{A} \\ -\frac{EA}{A} & \frac{EA}{L} \end{bmatrix} \quad (8)$$

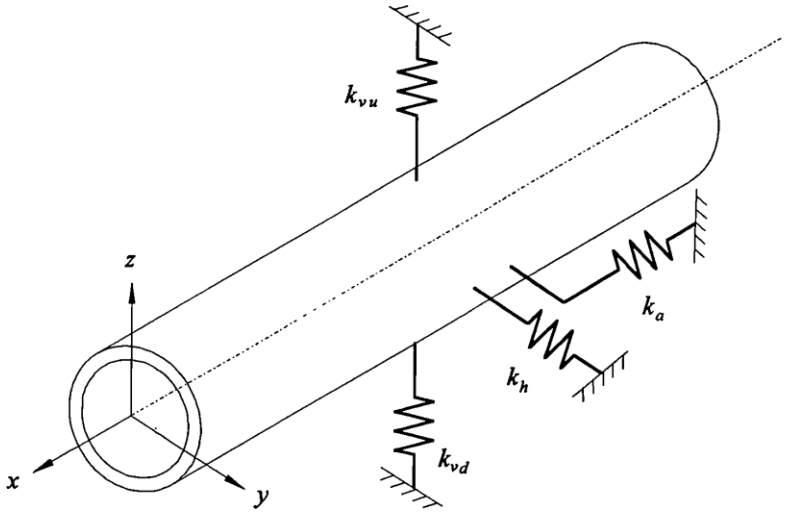


**Fig. 4.** Design scheme of the soil massif around the pipeline modeled by means of PLAXIS 3D and lateral stiffness matrix and lateral stiffness matrix

$$[K_{-p,lateral}] = \frac{EI}{L^3}\begin{bmatrix} 12 & 6L & -12 & 6L \\ 6L & 4L^2 & -6L & 2L^2 \\ -12 & -6L & 12 & -6L \\ 6L & 2L^2 & -6L & 4L^2 \end{bmatrix} \quad (9)$$

For one element, the total stiffness matrix is written as

$$[K_p] = \frac{EI}{L^3}\begin{bmatrix} \frac{L^2A}{I} & 0 & 0 & -\frac{L^2A}{I} & 0 & 0 \\ 0 & 12 & 6L & 0 & -12 & 6L \\ 0 & 6L & 4L^2 & 0 & -6L & 2L^2 \\ -\frac{L^2A}{I} & 0 & 0 & \frac{L^2A}{I} & 0 & 0 \\ 0 & -12 & -6L & 0 & 12 & -6L \\ 0 & 6L & 2L^2 & 0 & -6L & 4L^2 \end{bmatrix} \quad (10)$$

## 5. NUMERICAL MODELING OF THE STRESS STATE OF PIPE IN THE 2D SYSTEMS

Three-dimensional modeling of the "pipe-soil" system was carried out using the Plaxis 3D and SAP 2000 programs. Both programs are based on the finite element method and are widely used in the calculation of structural and engineering-geological projects. The calculations were carried out under conditions of spatial deformation. First, a manhole and a pipe system attached to it were designed. Two layers of soil with a total height of up to 30 m were taken under the structure. The connecting sewer pipes were modeled using the SAP2000 program.

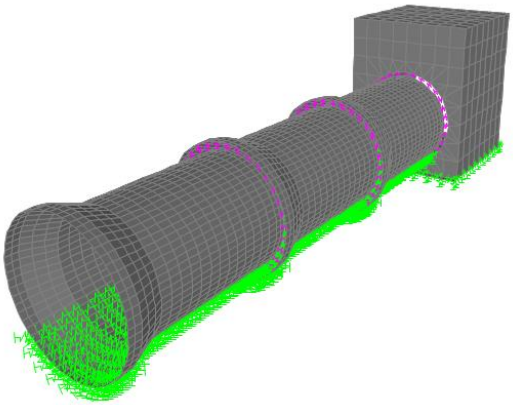

**Fig. 5.** Pipeline modeling according to the program SAP2000

The calculation took into account the weight of the overlying soil, the weight of the road surface, static and dynamic loads from transport, as well as horizontal seismic effects on the pipeline. 4272 quadrangular membrane elements and 4438 nodal points were used in the calculation. The stresses for a reinforced are shown in table 1.

**Table 1**

| N | Type of pipe | Maximum tension stress $\sigma^+$ , MPa | Maximum compression stress $\sigma^-$ , MPa |
|---|---|---|---|
| 1 | Reinforced concrete pipe | 20 | 20 |
| 2 | Fiberconcrete pipe with steel fibers | 17 | 17 |
| 3 | Fiberconcrete pipe with polypropilene fibers | 14 | 14 |

## CONCLUSION

1) Low stress values in fiber-reinforced concrete pipes compared to reinforced concrete pipes are the result of late cracking.

2) With an increase in the diameter and accordingly the weight of the pipe, the horizontal and vertical displacement increases. In this regard, for large-diameter pipelines, structural measures are necessary under the base of the pipeline.

3) Numerical modeling of the dynamic behavior of the pipeline under seismic impact revealed the sensitivity of the connection between the pipeline and the soil mass, which is included in the overall stiffness system of the pipeline.

4) The results of the study on the effect of the transverse component of the seismic load on the stress-strain state of the fiber-reinforced concrete pipe were included in the Technical Conditions developed by Evrascon Co.

## REFERENCES

[1] ASCE 27-00. Standart Practice design of precast concrete pipe for jacking in trenchless construction. ASCE. Reston, VA. 2000. 6211

[2] B.Kliszczewicz. Numerical 3D analysis of buried flexible pipeline. Eurepean scientific Journal Dec.2013. Ed.Vol.9.No 36.1857-7431

[3] D.F.Yosife, A.H.Aldefac, S.L.Zubaidi, A.N.Aldeflee. Numerical modelling of underground water pipelines exposed to seismic loading. Wasit Journal of Engineering Sciences. 2021, 9(2)

[4] Hongrhi Zhang. Seismic response of pipeline systems in a soil liquefaction environment. Old Dominion University. Winter. Virginia.1992

[5] Leach G., Harrold S. International collaborative research on soil / pipe interaction // Proceedings of the 2001 International Gas Research Conference, IGRC 2001, Amsterdam, 2001. Pp. 393-397.

[6] Nile B.K., Shaban A.M. Investigating lateral soil-sewer pipe displacements under inderect horizontal loads. ARPN Journal of Engineering and Applied Sciences. Vol.14, No.1, January.2019

[7] Paul Chi Fai Ng. Behavior if buried pipelines structured ti external loading. Thesis submitted to the University of Sheffield for the Degree of Doctor philosophy. November.1994

[8] R.A.Gumerov and ets. Estimation of lateral loads effect on the underground pipeline at seismic impact. Problem of collecting, preparing and transporting oil and oil products, 4(6) 2016. Moscow.Russia

[9] Technical Rules in Evrascon ASC "TS AZ 1000085511.002-2020. Underground fiber concrete free-flow sewerage pipes" 2020. Azerbaijan Certification Institute (ASI). State registration number No. 1955. (in Azerbaijani).

Azerbaijan University of Architecture and Construction
ISSN 2706-7726
Engineering Mechanics
Scientific and Technical Journal
E-mail: engineeringmechanics@azmiu.edu.az

| September 2023 | Issue 14 | Volume 6 | Number 2 | Pages 51-55 |
|---|---|---|---|---|

# DETERMINATION OF THE KINEMATIC CHARACTERISTICS OF MOVEMENT OF MACHINE AND EQUIPMENT PARTS

**SULEYMANOV T.S., ORUJOV Y.A., MAMMADOV F.KH., SALIMOVA E.N.**

fazil.adnsu@mail.ru, tahir_suleymanov@list.ru, elnare.selimova.1980@mail.ru

**Abstract.** *This work explores solution of a one-dimensional problem about propagation of harmonic waves in an orthotropic elastic tube containing heterogeneous incompressible liquid,* rheological behaviour of which is described by Maxwell model.

**Keywords:** *friction, rolling, relative motion, absolute motion, center of instantaneous velocities, angular velocity, axis of instantaneous velocities.*

**Introduction:** In the problem we are considering, object $A$ is rolling without friction around a stationary object $B$. So, when the object $A$ rotates around the fixed $OZ$ axis, the translational motion is absolute around the $O\Omega$ axis, and relative around the $O\zeta$ axis (figure 1).

It is known that the axes that change their position over time in the movement of rotation in space are called instantaneous rotation axes. The geometric meaning of the axes of rotation means that the velocity of the points taken on them at the moment of observation is zero. In this case, the object's angular velocity vector is viewed as a vector that shifts around the instantaneous rotation axis [1].

**Problem statement:** Assume that a spherical body $A$ rotates touching the inner surface of a stationary spherical body $B$. Let's determine the angular speed and angular momentum of body $A$, and at the same time, the speed and momentum of point $M$ located on body $A$, at a given moment, without considering the force of sliding - friction.

Let us assume that the angle between the generators of the $A$ -cone is α, the angle between the generators of the $B$-cone is $\beta$, $OM_0 = l$, $MM_0 = b$ –the $O\zeta$ axis of the body rotates with $\alpha$ – constant angular velocity $\omega_1$ - around the fixed $OZ$ axis.

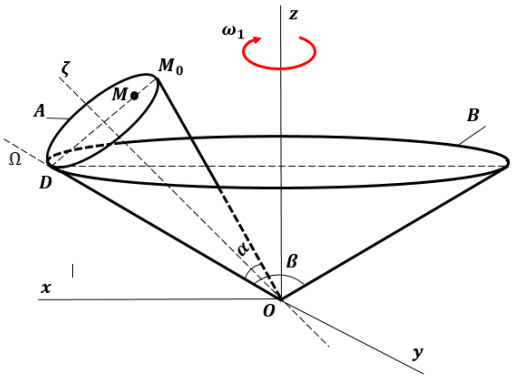

Figure 1. Spherical objects

**Solution method:** To determine the velocity of point $M$ located on the object $A$ it is necessary to first determine the angular velocity of the object $A$. For this, we will determine the speed of point $C$ on the $O\zeta$ axis of body $A$ based on the center of instantaneous velocities on the axes of instantaneous rotation. Circles with radius $CK_1$ are drawn around the point $C$ - axis $OZ$, and circles with radius $CK$ - around the axis $O\Omega$. Velocity vectors $\vec{v}_C$ and $\vec{v}_M$ are parallel to each other and the $OY$ axis and are perpendicular to the radius $CK$ and $CK_2$ (Figure 2).

Absolute velocity of point $C$ with respect to the center of instantaneous velocities $K$

$$v_C^m = \omega \cdot CK \tag{1}$$

The transfer speed of point $C$ according to the center of instantaneous velocities $K_1$ is as follows.

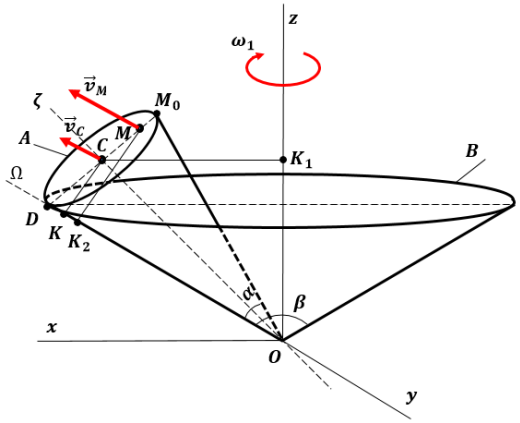


Figure 2. İllustration of the velocity of point M

$$v_C^e = \omega_1 \cdot CK_1 \tag{2}$$

To find the piece $CK$, first find $OC$ from $\Delta OCM_O$

$$OC = OM_O \cdot cos\frac{\alpha}{2} = l \cdot cos\frac{\alpha}{2}$$

$\Delta OCK$– from

$$CK = OC \cdot sin\frac{\alpha}{2} = l \cdot cos\frac{\alpha}{2} \cdot sin\frac{\alpha}{2} = \frac{1}{2} l \cdot sin\alpha$$

$\Delta\, OCK_1$– from

$$CK_1 = OC \cdot \sin\left(\frac{\beta}{2} - \frac{\alpha}{2}\right) = l \cdot cos\frac{\alpha}{2} \cdot \sin\left(\frac{\beta-\alpha}{2}\right)$$

$\Delta OCD$– from

$$DC = CM_0 = OD \cdot sin\frac{\alpha}{2} = l \cdot sin\frac{\alpha}{2}$$

$\Delta\, DMK_2$– from

$$\frac{MK_2}{MD} = sin\angle MDK_2 = sin\frac{180-\alpha}{2}$$

$$MK_2 = MD \cdot sin\frac{180-\alpha}{2} = (2DC - MM_O) \cdot sin\frac{180-\alpha}{2} = (2l \cdot sin\frac{\alpha}{2} - b) \cdot \cos\frac{\alpha}{2}$$

From (2), let's write the speed of point $C$ with respect to the $OZ$ axis as follows.

$$v_C^e = \omega_1 \cdot CK_1 = \omega_1 \cdot l \cdot cos\frac{\alpha}{2} \cdot \sin\left(\frac{\beta-\alpha}{2}\right) \tag{3}$$

From (1), the angular velocity of body $A$ with respect to the $O\Omega$ axis will be as follows.

$$\omega = \frac{v_C^e}{CK} = \frac{\omega_1 \cdot l \cdot cos\frac{\alpha}{2} \cdot \sin\left(\frac{\beta}{2} - \frac{\alpha}{2}\right)}{\frac{1}{2} l \cdot sin\alpha} \tag{4}$$

After finding the angular velocity of object $A$ with respect to the $O\Omega$ axis, we can also find the velocity of point $M$ (figure 3).

$$v_M^m = \omega \cdot MK_2 = \omega \cdot \left(2l \cdot sin\frac{\alpha}{2} - b\right) \cdot \cos\frac{\alpha}{2} = \omega \cdot \left(2l \cdot sin\frac{\alpha}{2}\cos\frac{\alpha}{2} - b\cos\frac{\alpha}{2}\right) = \omega \cdot (l \cdot sin\alpha - bcos\frac{\alpha}{2})$$

(5)

The direction of the angular velocity $\omega$ is determined based on the direction of the velocity $\vec{v}_C$ of point .

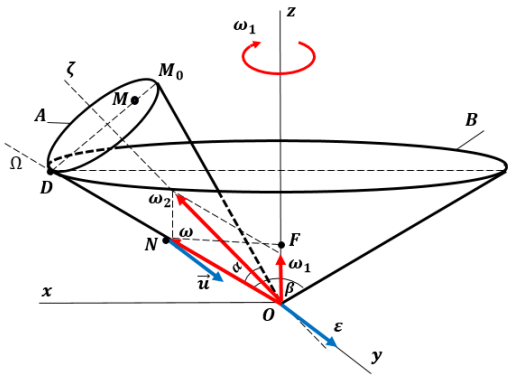


Figure 3. Illustration of instantaneous rotation axes

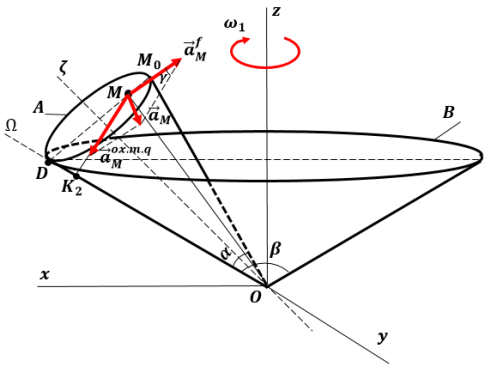


Figure 4. Illustration of the momentum of point $M$

$\omega$ - angular velocity can also be determined through the geometric sum of the angular powers established on the axes of instantaneous rotation intersecting at a point [3].

According to the theorem of sines, the angular velocities can be defined as follows.

$$\frac{\omega_1}{sin\frac{\alpha}{2}} = \frac{\omega}{\sin(\frac{\beta}{2} - \frac{\alpha}{2})} = \frac{\omega_2}{\sin(180^0 - \frac{\alpha+\beta}{2})} \quad (6)$$

$$\omega = \frac{\omega_1 \cdot \sin(\frac{\beta}{2} - \frac{\alpha}{2})}{sin\frac{\alpha}{2}}$$

From (6) we find $\omega_2$.

$$\omega_2 = \frac{\omega_1 \cdot sin\frac{\alpha+\beta}{2}}{sin\frac{\alpha}{2}} \quad (7)$$

$\omega_1$ is the angular velocity of the body $A$ rotating around its axis $OZ$.

$\omega_2$ is the angular velocity resulting from the rotation of body $A$ around its axis $O\zeta$.

Geometrically, the angular acceleration of the body $A$ is directed from the center $O$ parallel to the $OY$ axis, i.e. perpendicular to the $ZOX$ plane, parallel to the $\bar{u}$ - vector of the circle formed by the radius $NF$ from the end of the angular velocity $\omega$ - and perpendicular to the radius $NF = \omega \cdot cos\frac{\beta}{2}$ (Fig. 4). It can be written knowing that $u = \varepsilon$.

$$\varepsilon = \omega \cdot sin\frac{\beta}{2} \cdot \omega_1 = \frac{\omega_1 \cdot \sin(\frac{\beta}{2} - \frac{\alpha}{2})}{sin\frac{\alpha}{2}} \cdot sin\frac{\beta}{2} \cdot \omega_1 \quad (8)$$

Note that when finding the momentum of point , Coriolis momentum does not arise. We know that Coriolis acceleration is vectorially $\vec{a}_k = 2\omega_1 \times \vec{v}_r$, and modularly $a_k = 2\omega_1 \cdot v_r \cdot \sin(\omega_1, v_r)$.

In the problem we are studying, the body $A$ rotates both around its own axis and about the stationary $OZ$ axis. But since there is no forward movement (because the relative speed of the forward movement is $\vec{v}_r = 0$ the coriolis momentum is equal to zero.

The momentum of the point $M$ - is equal to the geometric sum of the momentum $\vec{a}_M^{ox.m.q}$ perpendicular to the $O\Omega$ axis and $\vec{a}_M^f$ perpendicular to the segment $OM$. That is, a_M, which is the diagonal of the parallelogram whose sides are $\vec{a}_M^{ox.m.q}$ and $\vec{a}_M^f$ is immediately determined. Note that , $\vec{a}_M$, $\vec{a}_M^{ox.m.q}$ and $\vec{a}_M^f$ are located on the $ZOX$ plane.

Let's write the following geometric curve

$$\vec{a}_M = \vec{a}_M^{ox.m.q} + \vec{a}_M^f \quad (9)$$

here is the centrifugal force relative to the axis

$$a_M^{ox.m.q} = \omega^2 \cdot MK_2 = \omega^2 \cdot \left(2l \cdot sin\frac{\alpha}{2} - b\right) \cdot \quad \cos\frac{\alpha}{2} \quad (10)$$

Rotational speed

$$a_M^f = \varepsilon \cdot OM \quad (11)$$

happens.

From $\Delta\, OMD$, we can find $OM$ according to the theorem of cosines.

$$OM = \sqrt{OD^2 + MD^2 - 2OD \cdot MD \cdot cos\frac{180^0 - \alpha}{2}} =$$

$$\sqrt{l^2 + (2DC - MM_O)^2 - 2l \cdot (2DC - MM_O) \cdot sin\frac{\alpha}{2}} =$$

$$\sqrt{l^2 + (2l \cdot sin\frac{\alpha}{2} - b)^2 - 2l \cdot (2l \cdot sin\frac{\alpha}{2} - b) \cdot sin\frac{\alpha}{2}} = \sqrt{l^2 - 2bl \cdot sin\frac{\alpha}{2} + b^2}$$

From formula (8).

$$a_M^f = \varepsilon \cdot \sqrt{l^2 - 2bl \cdot sin\frac{\alpha}{2} + b^2} \quad (12)$$

happens.

We can find the value of $\vec{a}_M$ from the parallelogram with sides $\vec{a}_M^{ox.m.q}$ and$\vec{a}_M^f$.

$$a_M = \sqrt{(a_M^{ox.m.q})^2 + (a_M^f)^2 - 2a_M^{ox.m.q} \cdot a_M^f \cdot cos\gamma} = \sqrt{(\omega^2(2lsin\frac{\alpha}{2} - b) \cdot$$

$$\cdot cos\frac{\alpha}{2})^2 + \left[\varepsilon \cdot \sqrt{l^2 - 2bl \cdot sin\frac{\alpha}{2} + b^2}\right]^2 - 2 \cdot \omega^2 \cdot \left(2l \cdot sin\frac{\alpha}{2} - b\right) \cdot$$

$$\cdot \cos\frac{\alpha}{2}\varepsilon \cdot \sqrt{l^2 - 2bl \cdot sin\frac{\alpha}{2} + b^2 cos\gamma} = \sqrt{\left[\frac{\omega^2 cos\frac{\alpha}{2}}{b}\left(2blsin\frac{\alpha}{2} - b^2\right)\right]^2 -$$

$$-\varepsilon^2\left[l^2 - \left(2blsin\frac{\alpha}{2} - b^2\right)\right] - \frac{2\varepsilon\omega^2 cos\frac{\alpha}{2}cos\gamma}{b} \cdot \left(2blsin\frac{\alpha}{2} - b^2\right) \cdot$$

$$\cdot \sqrt{l^2 - \left(2blsin\frac{\alpha}{2} - b^2\right)}$$

If we substitute $2blsin\frac{\alpha}{2} - b^2 = t$, as a result we will find the momentum of point $M$.

$$a_M = \sqrt{\left[\frac{\omega^2 cos\frac{\alpha}{2}}{b} \cdot t\right]^2 - \varepsilon^2[l^2 - t] - \frac{2\varepsilon\omega^2 cos\frac{\alpha}{2}cos\gamma}{b} \cdot t \cdot \sqrt{l^2 - t}} \qquad (13)$$

## CONCLUSIONS

The absolute velocity and absolute acceleration of an arbitrary point taken on the object during the rotation movement of the solid body around two intersecting axes during non-slip rolling are determined.

## REFERENCES

1. Kerimov O.M. Short course of theoretical mechanics, Baku, Azerneshr, 2011, 473 P.
2. Suleymanov T.S., Ibragimov J.X. Methods of approximate solution of problems of theoretical mechanics, Baku, 2020, 400 P.
3. Yablonsky A.A. Course of theoretical mechanics, M., Higher School, part II, 1984. 423 p.
4. T.V. Druzhinina, A.A. Mironenko Methodology for solving kinematics problems 620002, Yekaterinburg, Mira str. 19. 41 p.

Azerbaijan University of Architecture and Construction
ISSN 2706-7726
Engineering Mechanics
Scientific and Technical Journal
E-mail: engineeringmechanics@azmiu.edu.az

| September 2023 | Issue 14 | Volume 6 | Number 2 | Pages 56-59 |
|---|---|---|---|---|

# FIBER CONCRETE BASED ON PLASTIC WASTE

**K.B. JAMALOVA, T.A.HAGVERDIEVA**
khayala.jamalova@azmiu.edu.az, tahira.haqverdiyeva@azmiu.edu.az

**Abstract.** *The feasibility of preparing fiber-reinforced concrete mixtures from polyethylene terephthalate-containing plastic waste has been studied. It has been established that fibers can be obtained from them and used in concrete. By using polyethylene terephthalate-containing plastic waste fibers, it is possible to obtain water-resistant, crack-resistant, abrasion-resistant concrete.*
***Key words:*** *heavy concrete, metal, polypropylene, waste based on polyethylene terephthalate, fiber-reinforced concrete, compressive strength, impact resistance, crack resistance, friction, waterproofing*

**Introduction.** Considering that concrete and reinforced concrete products are one of the main building materials used in construction today, one can see the fundamental influence of the concrete mixture and the quality of products made on its basis on a number of indicators of buildings being built. and amenities. Currently, concrete mixtures for various purposes are used in construction. Recently, the use of reinforced concrete (fiber-reinforced concrete) with various fibers has been expanding in the construction of buildings and structures of special importance that have specific properties. That is why the field of application of fiber-reinforced concrete was initially investigated [1].

Based on the results of an analysis of the development and improvement of concrete and structures, it should be noted that fiber-reinforced concrete is one of the promising building materials of the 21st century. The world's first patent for a fiber-reinforced concrete structure was received by Russian scientist V.P. Nekrasov. in 1909, and research on the development of fiber-reinforced concrete and methods for calculating structures made from them has been widely developed since the 60s of the 20th century. Since then, a significant number of international scientific and technical symposiums, conferences and seminars have been held on the results of scientific research and the practical application of fiber-reinforced concrete in construction abroad [2].

By adding 1.6% fiber reinforcement (steel fiber) to concrete, its compressive strength can be increased to 35%, and its flexural strength by 2.4 times, and the percentage of fiber reinforcement has been studied to have a great influence on the properties concrete mixture and concrete [3].

The crack resistance index of fiber-reinforced concrete with and without additives was determined. Based on the test result, it was determined that the crack resistance index was higher for concrete samples using polypropylene and metal fibers than for conventional concrete. In fiber-reinforced concrete using microsilica, the strength properties have improved. The effectiveness of using such concretes in the construction of road surfaces has been established [4].

Scientific research has shown that industrial and household waste is a cheap source of raw materials for the building materials industry. Household waste from containers used by the population to store carbonated and non-carbonated drinks is thrown into trash cans. Such waste significantly worsens the environmental situation. If we take into account that the disposal of this waste is not allowed, it does not rot, and when burned, toxic substances are released into the air, then the possibility of

using such waste in other areas becomes an urgent issue. In this regard, the purpose of this research work was to study the possibility of using plastic containers for various carbonated and non-carbonated drinks, widely used in households, in concrete production. Polyethylene terephthalate-containing plastic containers used for storing carbonated and non-carbonated drinks were used. For the first time, polyethylene terephthalate was purchased as a synthetic fiber by British Calico Printers (England) in 1941. The copyright for the use of the new material was acquired by DuPont and ICI, which in turn sold licenses for the use of polyethylene terephthalate fiber to many other companies. A typical half-liter polyethylene terephthalate container weighs about 28 g, and a standard container of the same volume weighs about 350 g. Polyethylene terephthalate and containers made from it are non-toxic under normal conditions and do not have a harmful effect on the human body. Therefore, polyethylene terephthalate containers have found the widest field of application in food packaging today [5,6].

Purpose of the work: The main goal of the work was to study the use of plastic industrial waste as fiber-reinforced concrete and determine performance indicators.

Materials and methodology used in the study. In the experiments, Holcim Expert 42.5 R cement produced in the Republic of Azerbaijan, sand from the Bahramtepe deposit and crushed stone from the Gudiyalchay quarry located in the Guba region, as well as fine sand were used as fine fillers. To regulate the properties of concrete, superplasticizer brand S520, hyperplasticizer brand HP777, polypropylene fibers brand SikaFiber PPM-12, metal 3D fibers with a diameter of 0.8 mm and fibers based on polyethylene terephthalate were used.

The tests were carried out in the Laboratory of Research and Testing of Building Materials of the Department of Materials Science of the Azerbaijan University of Architecture and Construction, the Ministry of Emergency Situations, the State Agency for Safety Control in Construction, as well as at the testing ground of S.A. Dadashev Research and Design Institute of Building Materials. Compressive strength of concrete on the hydraulic press UTEST UTS-4320 according to the EN 12390-2 standard, bending strength on the TsD-40 press according to the GOST 10180-90 standard, tensile strength on the GRM-2A press according to the GOST 10180-90 standard, for dynamic stability In a copy machine of the PMA-F brand, friction resistance is determined in the LKI-3M friction device according to GOST 13087-81, and water resistance is determined in UDF-6/04 No. 195. device according to AZS 572.5-2011 standard.

Execution and resolution of the case. Plastic household waste is crushed into lengths of 6 and 12 cm. When preparing a concrete mixture, a mixture was prepared using different amounts of fibers (Table 1) and the ease of shrinkage was determined. Based on the prepared concrete mixture, standard samples were prepared and tested after hardening under normal conditions. The test results of prepared fiber-reinforced concrete samples were compared with the test results of heavy concrete. The test results are shown in Table 1.

Table 1.

Physico-mechanical properties of concrete samples reinforced with various fibers

| № | Concrete type | The amount of fiber kg per 1m3 | Physical and mechanical properties | | | |
|---|---|---|---|---|---|---|
| | | | average density, kq/m3 | | compressive strength limit, MPa | |
| | | | sample | average limit | sample | average limit |
| 1 | Heavy concrete | 0 | 2000 | 2096 | 31,40 | 32,70 |
| | | | 2100 | | 32,50 | |
| | | | 2190 | | 34,20 | |
| 2 | Metal fiber reinforced concrete | 20 | 2348 | 2360 | 41,69 | 41,83 |
| | | | 2365 | | 41,85 | |
| | | | 2368 | | 41,97 | |
| | | 30 | 2338 | 2381 | 42,00 | 42,00 |
| | | | 2412 | | 42,80 | |

| | | | | | | |
|---|---|---|---|---|---|---|
| | | | 2354 | | 42,21 | |
| | | 45 | 2368 | 2370 | 41,90 | 41,96 |
| | | | 2370 | | 41,98 | |
| | | | 2373 | | 43,00 | |
| 3 | Polypropylene fiber reinforced concrete | 2 | 2362 | 2379 | 42,89 | 42,90 |
| | | | 2385 | | 42,94 | |
| | | | 2390 | | 42,87 | |
| | | 6 | 2384 | 2391 | 43,65 | 43,53 |
| | | | 2390 | | 43,54 | |
| | | | 2400 | | 43,41 | |
| | | 8 | 2369 | 2390 | 43,20 | 43,46 |
| | | | 2398 | | 43,50 | |
| | | | 2405 | | 43,69 | |
| 4 | Fiber-reinforced concrete from waste based on polyethylene terephthalate | 2 | 2348 | 2250 | 40,47 | 40,65 |
| | | | 2365 | | 40,81 | |
| | | | 2368 | | 40,68 | |
| | | 6 | 2365 | 2310 | 41,12 | 41,48 |
| | | | 2372 | | 41,96 | |
| | | | 2375 | | 41,36 | |
| | | 8 | 2343 | 2295 | 40,00 | 40,25 |
| | | | 2359 | | 40,45 | |
| | | | 2394 | | 40,31 | |
| | | 10 | 2362 | 2215 | 38,80 | 38,90 |
| | | | 2349 | | 38,99 | |
| | | | 2354 | | 38,92 | |

As can be seen from the table, when adding 30 kg of metal fiber per 1 m3 of concrete mixture, the compressive strength was 42 MPa, when adding 6 kg of polypropylene fiber - 43.53 MPa, and when adding 6 kg of polyethylene terephthalate-based fiber, it was 41.48 MPa. The test results of fiber-reinforced concrete samples were compared with the results of heavy concrete. The average density and compressive strength of metal fiber reinforced concrete are 13.59% and 28.44% respectively compared to heavy concrete, the average density and compressive strength of polypropylene fiber reinforced concrete are 14.07% respectively compared to heavy concrete. At the limit of 33.11%, polyethylene terephthalate waste fiber reinforced concrete increased by 10.21% and 26.85%, respectively, compared to heavy concrete. Comparison with the test results of concrete samples made from fiber-reinforced concrete, other metal and polypropylene fibers using fibers made from waste containing polyethylene terephthalate shows that it is possible to use fibers made from waste in the production of fiber-reinforced concrete. In order to determine the scope of application of fiber-reinforced concrete based on waste containing polyethylene terephthalate, experiments were carried out and performance indicators were determined.

The wear indicators of fiber-reinforced concrete samples molded using fibers made from prepared polyethylene terephthalate-containing plastic waste were studied. According to laboratory experiments, after 4 eating cycles, the average weight loss of the samples was 13.65 g, and the average resistance to abrasion and eating was 0.27 g/cm2. Compared to conventional concrete, the increase in corrosion resistance was 12.05%.

In the following experiments, the impact resistance of fiber-reinforced concrete samples made from waste plastic fibers containing polyethylene terephthalate was studied. It has been established that the first crack in such concrete samples appears on average after the 11th blow, and its destruction occurs after the 22nd blow. It is 5% stronger than ordinary concrete. The water resistance of the samples was investigated. Based on the results of the experiment, it was established that such concrete belongs to category W5.

## CONCLUSION

Test results indicate that fibers made from polyethylene terephthalate beverage bottles can be used in concrete production. It is possible to use fiber-reinforced concrete made with such fibers in the production of products in accordance with performance indicators.

## REFERENCES

1. Morozov V.I., Bakhotsky I.V. To the calculation of fiber-reinforced concrete structures subjected to combined effects of torsion and bending. Modern problems of science and education. No. 5, 2013. 109 p.
2. http://www.stroyunihim.ru/Armiruyushie-dobavki-v-beton/2013-04-03-15-54-58
3. Yusifov I.M. Technology of concrete and reinforced concrete products: Maarif Publishing House. Baku-1998. 388 pages. 60 rub.
4. Akhverdieva T.A., K.B. Jamalova. Study of the influence of additives on the properties of fiber-reinforced concrete. Concrete technologies. Moscow, No. 4, July 2023. pp. 25-29
5. Based on materials from the magazine "Industrial Encyclopedia". PET bottles: history, properties, production technology.
6. K.B. Jamalova. Possible use in production from household waste. International Center for Scientific Cooperation "Science and Enlightenment". Modern technologies: Current issues of theory and practice. Collection of articles of the V International Scientific and Practical Conference, held in VG. Penza. May 30, 2023 st. 29-31

Azerbaijan University of Architecture and Construction
ISSN 2706-7726
Engineering Mechanics
Scientific and Technical Journal
E-mail: engineeringmechanics@azmiu.edu.az

| September 2023 | Issue 14 | Volume 6 | Number 2 | Pages 60-64 |
|---|---|---|---|---|

# STEADY-STATE OSCILLATIONS OF VISCOUS-DAMAGED BAR WITH REGARD TO SECONDARY EFFECTS

**M.A.MAMMADOVA**
*Mechanics and mechanical engineering, "Mechanics of deformable solids" department,*
*Institute of Mathematics and Mechanics,*
meri.mammadova@gmail.com

**Abstract.** *Study of oscillations of mechanical systems with complex rheological properties, as a rule, is reduced to complex mathematical problems. It is impossible to solve these problems analytically and therefore the only way to solve them is numerical. But it sometimes limits visibility of the obtained solutions and does not allow to use them widely in practice, because the needs for engineering require relatively simple, closed formulas. To this end, approximate accounting of multi-dimensionality with the construction of quasi-one-dimensional model, generally speaking for multi-dimensional problem is actual. One of these ways is the rod bending model where the transverse motion inertia is taken into account in the form of additional term. The paper uses this method and studies flexural oscillations of visco-damaged rod in the absence of the effect of healing defects. A hereditary damageability model is taken as a model of damaged model.*
**Keywords:***oscillations, damageability, inertia of transverse motion, amplitude-frequency characteristics.*

## INTRODUCTION

In engineering and industry, flexural oscillations are the most common along with longitudinal oscillations. In [3], flexural oscillations of a finite length hereditary elastic rod was studied when a weakly-singular Abel kernel was taken as a creep core. Resonance frequencies were calculated for the values of the parameter $\alpha$ of Abel's core close to a unit.

Damageability is one the factors necessarily taken into account when calculating structural elements for strength and durability. Under variable loads this factor may be very influential. In the paper hereditary theory of damageability [4] is used. In one-dimensional statement the physical relation of this theory is of the form:

$$\varepsilon(t)=\frac{1}{E}\left\{\sigma(t)+\sum_{k=1}^{n}\Phi_k\left(t_k^+\right)\int_{t_k^-}^{t_k^+}K\left(t_k^+-\tau\right)\sigma(\tau)d\tau+\int_{t_{n+1}^-}^{t}K(t-\tau)\sigma(\tau)d\tau\right\}. \tag{1.1}$$

Here $K(t-\tau)$ is a changeability operator core that may be written briefly as:

$$K^*\sigma=\sum_{k=1}^{n}\Phi_k\left(t_k^+\right)\int_{t_k^-}^{t_k^+}K\left(t_k^+-\tau\right)\sigma(\tau)d\tau+\int_{t_{n+1}^-}^{t}K(t-\tau)\sigma(\tau)d\tau\,. \tag{1.2}$$

$\Phi_k\left(t_k^+\right)$ is a deficiency healing function dependent of the deficiency volume load accumulated during active loading $\left(t_k^-;t_k^+\right)$. The value $\Phi_k\left(t_k^+\right)=0$ corresponds to complete healing of deficiencies, the value $\Phi_k\left(t_k^+\right)=1$ corresponds to the absence of such a phenomenon.

Allowing for denotation (1.2), from (1.1) we get:

$$\varepsilon(t)=\frac{1}{E}\left\{\sigma(t)+K^{*}\sigma(t)\right\} \tag{1.3}$$

or

$$\varepsilon(t)=\frac{1}{E}\left(1+K^{*}\right)\sigma(t) \tag{1.4}$$

having denoted

$$\frac{1}{\widetilde{E}}=\frac{1}{E}(1+K^{*}) \tag{1.5}$$

to formula (1.3) we give the form

$$\varepsilon=\frac{1}{\widetilde{E}}\sigma.$$

In the sequel, we will assume the absence of deficiency healing phenomenon. Then the damageability operator (1.2) is of ordinary character of integral operator of hereditary theory of elasticity and all corresponding methods and laws of linear viscoelasticity may be applied to it.

In the paper we study a problem of flexural oscillations but with regard to rotation inertia of the element of a rod around the axis perpendicular to the rod flexion plane. For flexural waves, such an equation has the form [2]:

$$\rho J=\frac{\partial^{4}W_{1}}{\partial x_{1}^{2}\partial t_{1}^{2}}=EJ\frac{\partial^{4}W_{1}}{\partial x_{1}^{4}}+\rho S\frac{\partial^{2}W_{1}}{\partial t_{1}^{2}}. \tag{1.6}$$

Here $W_1$ is rod's flexure, $x_1$ is a longitudinal coordinate, $\rho$ is the density, $S$ is square of cross-section, $E$ is Young's modulus, $J=r_0^2S$ is inertia moment of rod's section, $r_0$ is radius of cross section inertia, that for circular transverse section equals $r_0=R/\sqrt{2}$ and $t_1$ is time.

**PROBLEM STATEMENT**

For obtaining appropriate equation of motion for a hereditary-elastic rod, to equation (1.6) we apply the Volterra-Rabotnov principle and get:

$$\frac{\rho r_0^2}{\widetilde{E}}\frac{\partial^{4}W_{1}}{\partial x_{1}^{2}\partial t_{1}^{2}}=r_0^2\frac{\partial^{4}W_{1}}{\partial x_{1}^{4}}+\frac{\rho}{\widetilde{E}}\frac{\partial^{2}W_{1}}{\partial t_{1}^{2}}\ , \tag{2.1}$$

where the operator $\widetilde{E}$ is determined according to (1.4). In this case we have:

$$-r_0^2\frac{\partial^{4}W_{1}}{\partial x_{1}^{2}\partial t_{1}^{2}}+\frac{\partial^{4}W_{1}}{\partial x_{1}^{4}}-r_0^2\frac{\partial^{2}}{\partial x_{1}^{2}}K^{*}\frac{\partial^{2}W_{1}}{\partial t_{1}^{2}}+K^{*}\frac{\partial^{2}W_{1}}{\partial t_{1}^{2}}+C_0^2r_0^2\frac{\partial^{4}W_{1}}{\partial x_{1}^{4}}=0$$

and as a creeping core we accept the Abel weakly-singular core:

$$I_{\alpha}=\frac{\beta}{\Gamma(1-\alpha)}t^{-\alpha},\ 0\le\alpha<1,$$

where $\Gamma(1-\alpha)$ is Euler's gamma-function .

We introduce the following pure variables:

$$x=\frac{x_1}{r_0};\qquad \eta=\frac{\beta r_0^{1-\alpha}}{C_0^{1-\alpha}},$$

where

$$C_0=\sqrt{\frac{E}{\rho}};\quad t=\frac{t_1C_0}{r_0};\quad W=\frac{W_1}{W_0}. \tag{2.2}$$

Then in pure variables we will have the following flexural oscillation equation:

$$-\frac{\partial^{4}W}{\partial x^{2}\partial t^{2}}+\frac{\partial^{2}W}{\partial t^{2}}+\frac{\eta}{\Gamma(1-\alpha)}\frac{\partial^{2}}{\partial x^{2}}\int_{-\infty}^{t}\frac{1}{(t-\tau)^{\alpha}}\frac{\partial^{2}W}{\partial\tau^{2}}d\tau-$$

$$-\frac{\eta}{\Gamma(1-\alpha)}\int_{-\infty}^{t}\frac{1}{(t-\tau)^{\alpha}}\frac{\partial^2 W}{\partial\tau^2}d\tau+\frac{\partial^4 W}{\partial x^4}=0 \tag{2.3}$$

The boundary conditions in pure variables, corresponding to the problem under consideration, will be:

$$W(0,t)=\cos\omega t;\qquad \frac{\partial^2 W}{\partial x^2}\Big|_{x=0}=0, \tag{2.4}$$

$$\frac{\partial^2 W}{\partial x^2}\Big|_{x=l/r_0}=\frac{\partial^3 W}{\partial x^3}\Big|_{x=l/r_0}=0 \tag{2.5}$$

The first two conditions of (2.4) correspond to no bending moment on the left end and giving on it forcing transverse osciallations with frequency $\omega$ and amplitude $W_0$. Boundary conditions (2.5) correspond to no forces on the right end of the rod, bending moment and intersecting force.

We will look for the solution of problem (2.3)-(2.5) in the form of a series:

$$W(x,t)=\sum_{k=1}^{\infty}W_k(x,\gamma_k)e^{-i\gamma_k t}. \tag{2.6}$$

Substituting representation (2.6) in (2.3), for the function $W_k(x,\gamma_k)$ we get the following ordinary differential equation of fourth order with constant complex coefficients of the form:

$$\frac{d^4 W_k}{dx^4}+\lambda_k^2\frac{d^2 W_k}{dx^2}-\lambda_k^2 W_k=0, \tag{2.7}$$

where

$$\lambda_k^2=\gamma_k^2\left(1-\eta\frac{i^{1-\alpha}}{\gamma_k^2}\right). \tag{2.8}$$

Finding the solution of equation (2.7) in the form $W_k=e^{P_k x}$ reduces to the following characteristic equation:

$$P_k^4+\lambda_k^2P_k^2-\lambda_k^2=0. \tag{2.9}$$

Here we consider two cases. The first case, when $\gamma_k>0$, then

$$\lambda_k^2=A_k-iE_k, \tag{2.10}$$

where

$$A_k=\gamma_k^2-\eta\gamma_k^{1+\alpha}\sin\frac{\pi\alpha}{2};\quad E_k=\eta\gamma_k^{1+\alpha}\cos\frac{\pi\alpha}{2}. \tag{2.11}$$

In the case $\gamma_k<0$ we get:

$$\lambda_k^2=A_k+iE_k. \tag{2.12}$$

The roots of the characteristic equation (2.9) for $\gamma_k>0$ will be:

$$\begin{gathered}
P_k^{(1)}=-P_k^{(2)}=S_k^{(1)}+i\rho_k^{(1)};\qquad P_k^{(3)}=-P_k^{(4)}=S_k^{(2)}-i\rho_k^{(2)};\\
S_k^{(n)}=\left[\left(r_k^{(n)}+\alpha_k^{(n)}\right)/2\right]^{\frac{1}{2}};\qquad \rho_k^{(n)}=\left[\left(r_k^{(n)}-\alpha_k^{(n)}\right)/2\right]^{\frac{1}{2}};\\
r_k^{(n)}=\sqrt{\alpha_k^{(n)2}+\beta_k^{(n)2}};\qquad r_k=\left(a_k^2+b_k^2\right)^{\frac{1}{2}};\\
\alpha_k^{(1)}=\frac{1}{2}\left(-A_k+\left[\left(r_k+a_k\right)/2\right]\right)^{\frac{1}{2}};\qquad \beta_k^{(1)}=\frac{1}{2}\left(E_k+\left[\left(r_k-a_k\right)/2\right]\right)^{\frac{1}{2}};\\
\alpha_k^{(2)}=-\frac{1}{2}\left(A_k+\left[\left(r_k+a_k\right)/2\right]\right)^{\frac{1}{2}};\qquad \beta_k^{(2)}=\frac{1}{2}\left(E_k-\left[\left(r_k-a_k\right)/2\right]\right)^{\frac{1}{2}};\\
a_k=A_k^2+4A_k-E_k^2;\qquad b_k=2A_kE_k+4E_k.
\end{gathered} \tag{2.13}$$

For $\gamma_k < 0$ the roots of equation (2.9) will be:

$$\begin{cases} P_k^{(1)} = -P_k^{(2)} = S_k^{(1)} - i\rho_k^{(1)}; \\ P_k^{(3)} = -P_k^{(4)} = S_k^{(2)} + i\rho_k^{(2)}. \end{cases} \tag{2.14}$$

Now we write the solution of differential equation (2.7) in the form:

$$W_k(x,\gamma_k) = C_k^{(1)} chP_k^{(1)} x + C_k^{(2)} chP_k^{(1)} x + C_k^{(3)} chP_k^{(3)} x + C_k^{(4)} chP_k^{(3)} x; \tag{2.15}$$

where the constants $C_k^{(n)}$, generally speaking, are complex and are determined from the boundary conditions. Proceeding from boundary conditions (2.4), (2.5) for the function $W_k(x,\gamma_k)$ we accept the following conditions:

$$W_k(0) = \frac{1}{2}; \qquad \frac{\partial^2 W_k}{\partial x^2}\Big|_{x=0} = 0; \tag{2.16}$$

$$\frac{\partial^2 W_k}{\partial x^2}\Big|_{x=\frac{1}{r_0}} = \frac{\partial^3 W_k}{\partial x^3}\Big|_{x=\frac{1}{r_0}} = 0.$$

When taking into account the expressions obtained for $W_k$ in (2.6), the boundary conditions (2.5) in the right end and the second one from boundary conditions (2.4) on the left end is fulfilled. It remains that the complete solution of (2.6) satisfy the remaining boundary condition (2.4). For that we are restricted in series (2.6) with two first terms having put $\gamma_1 = \omega; \gamma_2 = -\omega$ . From the same representation (2.6) we see that the remaining boundary condition (2.4) is fulfilled:

$$W(0,t) = W_1(0)e^{-i\omega t} + W_2(0)e^{i\omega t} = \frac{1}{2}\left(e^{-i\omega t} + e^{i\omega t}\right) = \cos\omega t \tag{2.17}$$

Then the solution (2.6) of differential equation (2.3) with boundary conditions (2.4), (2.5) will be obtained in the form:

$$W(x,t) = W_1(x,\omega)e^{-i\omega t} + W_2(x,-\omega)e^{i\omega t} \tag{2.18}$$

or in a compact form convenient for practical use:

$$W(x,t) = 2R(x,\omega)\cos\left[\omega t - \theta(x,\omega)\right]. \tag{2.19}$$

The expression obtained for the dependence of amplitude $R$ from frequency $\omega$ has a very bulky form. Bur for a great majority of real materials it can be simplified. For many materials the singularity index of Abel's core $\alpha$ is very close to a unit. Then we have:

$$\begin{cases} A = \omega^2 - \eta\omega^{1+\alpha}; \quad E = 0 \\ a = \left(\omega^2 - \eta\omega^{1+\alpha}\right)^2 + \left(\omega^2 - \eta\omega^{1+\alpha}\right); \quad b = 0 \\ \alpha^{(1)} = \frac{1}{2}\left[ a^{\frac{1}{2}} - \left(\omega^2 - \eta\omega^{1+\alpha}\right); \quad \beta^{(1)} = 0 \right. \\ \alpha^{(2)} = \frac{1}{2}\left[ a^{\frac{1}{2}} + \left(\omega^2 - \eta\omega^{1+\alpha}\right); \quad \beta^{(2)} = 0 \right. \\ r^{(n)} = \alpha^{(n)}; \quad S^{(m)} = \sqrt{\alpha^{(m)}}; \quad \rho^{(n)} = 0. \end{cases} \tag{2.20}$$

$$P^{(1)} = -P^{(2)} = \sqrt{\alpha^{(1)}}; \qquad P^{(3)} = -P^{(n)} = \sqrt{\alpha^{(2)}}. \tag{2.21}$$

For oscillation amplitude we get the following simplified expression:

$$2R =_1 sh\sqrt{\alpha^{(1)}}\, x + \phi_2 ch\sqrt{\alpha^{(1)}}\, x + \phi_3 sh\sqrt{\alpha^{(2)}}\, x + \phi_4 ch\sqrt{\alpha^{(2)}}\, x, \tag{2.22}$$

where

$$\phi_1 = \frac{\left\{\sqrt{\alpha^{(2)}} + \sqrt{\alpha^{(1)}} sh\sqrt{\alpha^{(1)}}\frac{1}{r_0} sh\sqrt{\alpha^{(2)}}\frac{1}{r_0} + \sqrt{\alpha^{(2)}} ch\sqrt{\alpha^{(1)}}\frac{1}{r_0} ch\sqrt{\alpha^{(2)}}\frac{1}{r_0}\right\}\alpha^{(2)}}{\left[\sqrt{\alpha^{(1)}} sh\sqrt{\alpha^{(2)}}\frac{1}{r_0} ch\sqrt{\alpha^{(1)}}\frac{1}{r_0} - \sqrt{\alpha^{(2)}} sh\sqrt{\alpha^{(1)}}\frac{1}{r_0} ch\sqrt{\alpha^{(2)}}\frac{1}{r_0}\right]\left(\alpha^{(1)} - \alpha^{(2)}\right)};$$

$$\phi_2 = \frac{\alpha^{(1)}}{\alpha^{(1)} - \alpha^{(2)}} \frac{\sqrt{\alpha^{(1)}} + \sqrt{\alpha^{(2)}} sh\sqrt{\alpha^{(1)}}\frac{1}{r_0} sh\sqrt{\alpha^{(2)}}\frac{1}{r_0} - \sqrt{\alpha^{(1)}} ch\sqrt{\alpha^{(1)}}\frac{1}{r_0} ch\sqrt{\alpha^{(2)}}\frac{1}{r_0}}{\sqrt{\alpha^{(1)}} sh\sqrt{\alpha^{(2)}}\frac{1}{r_0} ch\sqrt{\alpha^{(1)}}\frac{1}{r_0} - \sqrt{\alpha^{(2)}} sh\sqrt{\alpha^{(1)}}\frac{1}{r_0} ch\sqrt{\alpha^{(2)}}\frac{1}{r_0}};$$

$$\phi_3 = -\frac{\alpha^{(2)}}{\alpha^{(1)} - \alpha^{(2)}}; \qquad \phi_4 = \frac{\alpha^{(1)}}{\alpha^{(1)} - \alpha^{(2)}}. \tag{2.23}$$

## NUMERICAL REALIZATION

The amplitude-frequency curves for force-free right end of the rod was constructed on the base of representation (2.22). Numerical realization was performed for the following values of the parameters:

$$\alpha = 0{,}7; \quad \beta\left(\frac{1}{\omega}\right)^{1-\alpha} = 0{,}1; \quad \delta = \frac{r_0}{l} = 0{,}001; \quad 0{,}01;\ 0{,}1.$$

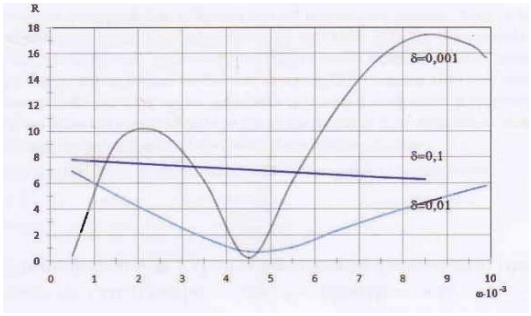


**Fig. 1.** Amplitude-frequency curves

## CONCLUSION

As we see from the graph, account of inertia of torsion of the rod's element with respect to the axis perpendicular to the flexure plane reduces to smoothing of the amplitude-frequency curve.

Within the studied frequencies, reduction of the parameter $\eta$ characterizing the torsion inertia from the value $5{,}13\cdot10^{-3}$ to $1{,}29\cdot10^{-3}$ leads to appearance of two brightly expressed resonance frequencies.

## REFERENCES

1. Л.М.Бреховских, В.В.Гончаров. Введение в механику сплошных сред. М., Наука, 1982, 335 с.
2. Ю.Н. Работнов Элементы наследственной механики твёрдых тел. М., Наука,1977, с.384.
3. Ю.В.Суворова. Нелинейно-наследственные модели деформирования и разрушения конструкционных материалов. Докторская диссертация. М. 1979, 399 с. ГНИИМАШ.
4. Ю.В.Суворова, М.Б.Ахундов Длительное разрушение изотропной среды в условиях сложного напряжённого состояния. Машиноведение. АН СССР, 1986, №4, с. 40-46.